[American Journal of Science, Vol. 311, January, 2011, P. 1–26, DOI 10.2475/01.2011.01]

American Journal of Science

JANUARY 2011

GEOLOGIC CONSTRAINTS ON THE GLACIAL AMPLIFICATION OF PHANEROZOIC CLIMATE SENSITIVITY

JEFFREY PARK* and DANA L. ROYER**

ABSTRACT. The long-term carbon cycle depends on many feedbacks. Silicate weathering consumes atmospheric CO_2, but is also enhanced by the increased temperatures brought about by this important greenhouse gas. The long-term sensitivity ΔT_{2x} of climate to CO_2-doubling modulates the strength of this negative feedback. We update the model-experiment of Royer and others (2007) by estimating an empirical probability-density function (PDF) of ΔT_{2x} for the Phanerozoic by using an improved GEOCARBSULF carbon-cycle model to predict a larger, recalibrated set of proxy-CO_2 measurements from the present-day to 420 Ma. The new GEOCARBSULF parameterizes the rapid weathering of volcanic rocks, relative to plutonic rocks. Updates to the carbon-cycle model and the proxy-CO_2 data set induce opposing model responses. As a result, our experiment maintains an agreement with ΔT_{2x} estimates based on numerical climate models and late Cenozoic paleoclimate. For a climate sensitivity ΔT_{2x} that is uniform throughout the Phanerozoic, the most probable value is 3° to 4 °C. GEOCARBSULF fits the proxy-CO_2 data equally well, and with far more parameter choices, if ΔT_{2x} is amplified by at least a factor of two during the glacial intervals of the Paleozoic (260-340 Ma) and Cenozoic (0-40 Ma), relative to non-glacial intervals of Earth history. For glacial amplification of two, the empirical PDFs for glacial climate sensitivity predict $\Delta T_{2x}^{(g)} > 2.0$ °C with ~99 percent probability, $\Delta T_{2x}^{(g)} > 3.4$ °C with ~95 percent probability, and $\Delta T_{2x}^{(g)} > 4.4$ °C with ~90 percent probability. The most probable values are $\Delta T_{2x}^{(g)} = 6°$ to 8 °C. This result supports the notion that the response of Earth's present-day surface temperature will be amplified by the millennial and longer-term waxing and waning of ice sheets.

Key words: Carbon cycle, Bayesian probability, climate sensitivity, glacial feedback, paleoclimate

INTRODUCTION

Correlations between atmospheric carbon dioxide and global temperatures have been found on time scales both historical (Hegerl and others, 2006; IPCC, 2007; Knutti and Hegerl, 2008) and geological (Budyko, 1974, 1982; Zubakov and Borzenkova, 1990; Berner, 1991; Hoffert and Covey, 1992; Borzenkova, 2003; Pagani and others, 2006, 2010; Royer and others, 2007; Knutti and Hegerl, 2008; Tong and others, 2009; Lunt and others, 2010). Climate sensitivity ΔT_{2x} scales a rise in global-average temperature to the doubling of atmospheric CO_2. The direct radiative effect of CO_2 is altered by feedbacks on both short and long time scales. Short-term ΔT_{2x} can be estimated with numerical climate models in which the radiation balance is manipulated to simulate an increase in greenhouse gasses. Uncertainties in feedback parameterizations lead to a range of ΔT_{2x} estimates that has remained remarkably stable over time: from 2° to 5.5 °C a century ago (Arrhenius, 1896), to 1.5° to 4.5 °C in the 1960s

* Department of Geology and Geophysics, Yale University, PO Box 208109, New Haven, Connecticut 06520-8109, U.S.A.; jeffrey.park@yale.edu

** Department of Earth and Environmental Sciences, Wesleyan University, Exley Science Center 445, Middletown, Connecticut 06459-0139 U.S.A.; droyer@wesleyan.edu

(Manabe and Wetherald, 1967), and currently 2.1° to 4.4 °C, based on both models and historical data (Randall and others, 2007).

Lunt and others (2010) defines an "Earth-system sensitivity" ΔT_{2x} that incorporates both slow feedbacks, for example, ice-sheet growth, and rapid feedbacks that involve threshold effects, for example, vegetation cover. Long-term feedbacks involving secular changes to the ocean, cryosphere and biosphere are difficult to represent with confidence using general circulation models with short time steps (Bala and others, 2006, 2007; Boe and others, 2009). A different type of estimate relates past climate observations to past CO_2 variations, either from historical measurements (Wigley and others, 1997) or from proxy and paleoclimate data (Siegenthaler and others, 2005; Hegerl and others, 2006; Pagani and others, 2006; Higgins and Schrag, 2006). A review by Knutti and Hegerl (2008) concludes that "studies that use information in a relatively complete manner generally find a most likely value between 2 °C and 3.5 °C" for the fast-feedback climate sensitivity, but that larger values of short-term ΔT_{2x} could not be excluded. Hansen and others (2008) estimated short-term ΔT_{2x}~3 °C, but argued that glacial amplification increased long-term ΔT_{2x} to 6 °C. Underscoring this last point, Pagani and others (2010) compared temperature and CO_2 changes between the present day and the Pliocene (4.5 Ma), just before the onset of major Northern Hemisphere ice sheets. Their estimated long-term ΔT_{2x} of 7 °C or more suggests that slow cryospheric feedbacks have the potential to amplify greatly the climate sensitivity to increased CO_2, a view echoed by Lunt and others (2010). Glacial amplification of enhanced-greenhouse climate response is an idea with some history, for example, Budyko (1974, 1982). Based on paleoclimate reconstructions, the "Method of Paleoanalogs" demonstrated large changes in high-latitude temperature in Earth's past, consistent with glacial amplification (Shabalova and Können, 1995; Kheshgi and others, 1997; Crowley, 1997).

Royer and others (2007) proposed an independent estimate of long-term climate sensitivity ΔT_{2x} based on the long-term GEOCARBSULF carbon-cycle model of the Phanerozoic (Berner, 2006a). GEOCARBSULF determines atmospheric CO_2 concentration under the assumption that carbon fluxes into, and out of, the surface-Earth system (atmosphere, soil, ocean, biosphere) are balanced on 10-My time scales. The weathering of silicate rocks increases with temperature, and temperature increases with atmospheric CO_2. Silicate weathering consumes CO_2 via carbonic acid and plant-derived acids (Moulton and others, 2000), and thus its dependence on temperature moderates the atmospheric CO_2 concentration. To balance the carbon flux into the surface environment from volcanic degassing, organic-carbon weathering and other factors, smaller excursions in atmospheric CO_2 over Earth history are necessary if ΔT_{2x} is large. Conversely, larger CO_2 excursions are required if ΔT_{2x} is small. Using this feedback, Phanerozoic proxy-CO_2 data from the present-day to 420 Ma (Royer, 2006, 2010) can be used to constrain the parameter ΔT_{2x} in the context of the GEOCARBSULF model. Because several other GEOCARBSULF parameters are imperfectly known, Royer and others (2007) explored plausible combinations of model parameters to identify which values permitted the model to represent proxy-CO_2 data within an acceptable misfit. At specified values of ΔT_{2x}, Royer and others (2007) aggregated all model-parameter choices that could fit the data within a specified tolerance, and constructed an empirical probability density function (PDF) for climate sensitivity. Their empirical PDF for ΔT_{2x} resembled more-direct estimates (Knutti and Hegerl, 2008): a most-probable ΔT_{2x} = 2.8 °C and 95 percent confidence (in a Bayesian sense) that 1.5 °C < ΔT_{2x} < 6.2 °C.

Three factors motivate an update of Royer and others (2007). The GEOCARBSULF model has been revised to reflect the weathering rates of volcanic Ca- and Mg-silicate rocks, which differ from plutonic silicates (Berner, 2006b). The proxy-CO_2 dataset has been expanded and recalibrated (Montañez and others, 2007; Fletcher and others, 2008; Cleveland and others, 2008; Breecker and others, 2009, 2010; Retallack, 2009b; Beerling and others, 2009; Pearson and others, 2009; Tripati and others, 2009; Royer, 2010), including age updates according to Gradstein and others (2004). Although the expansion and interpretation of the proxy-CO_2 data set is ongoing, this study incorporates ~50 percent more data than were considered by Royer and others (2007), allowing better resolution of carbon-cycle history. Comparison with a larger data set can identify Earth-history intervals where data and/or the model may be uncertain or incorrect. The correlations between climate-sensitivity and other parameters in the carbon-cycle model GEOCARBSULF were not explored in detail by Royer and others (2007). Finally, we evaluate the possibility of enhanced ice-sheet feedback (Budyko, 1974; Hansen and others, 2008; Pagani and others, 2010; Lunt and others, 2010) by allowing GEOCARBSULF climate sensitivity ΔT_{2x} to have independent values in glacial and non-glacial periods of the Phanerozoic. The GEOCARBSULF Carbon-Cycle Model section discusses the background of the GEOCARBSULF carbon-cycle model. The Proxy-CO_2 Data and Bayesian Modeling section discusses proxy-CO_2 measurements used to constrain the GEOCARBSULF parameters, as well as the Bayesian statistical assumptions behind the empirical PDF for ΔT_{2x}. The Climate Sensitivity and Parameter Tradeoffs section updates the Royer and others (2007) study for Phanerozoic climate sensitivity. The Data Fitting and Discussion section discusses the results, and considers how to improve the carbon-cycle approach to ΔT_{2x}-estimation.

THE GEOCARBSULF CARBON-CYCLE MODEL

The BLAG model (Berner and others, 1983) fired an early shot in the earth-system revolution by integrating through time the environmental influence of four generalized chemical reactions,

$$CO_2 + CaSiO_3 \Leftrightarrow CaCO_3 + SiO_2$$

$$CO_2 + MgSiO_3 \Leftrightarrow MgCO_3 + SiO_2$$

$$CO_2 + H_2O \Leftrightarrow CH_2O + O_2$$

$$4FeS_2 + 15O_2 + 8H_2O \Leftrightarrow 2Fe_2O_3 + 8H_2SO_4$$

The first two (Urey) reactions symbolically represent the exchange between global inventories of silicate and carbonate rocks via weathering and metamorphism (Ebelmen, 1845). The third reaction represents the formation and net burial, or release, of organic carbon in the earth system. The fourth reaction represents the global exchange between sulfides and sulfates. These reactions codify a suite of geologic processes that govern the atmospheric concentration of CO_2 and O_2 through Earth history. Because CO_2 is a major greenhouse gas and O_2 is necessary for respiration, the history of these gasses in Earth's atmosphere is a major factor in Earth's climate history (Royer and others, 2004; Royer, 2006; Fletcher and others, 2008) and biological evolution (Falkowski and others, 2005; Berner and others, 2007; Franks and Beerling, 2009). By integrating a system of differential equations for geochemical cycles through time with hypothetical plate-tectonic histories, Berner and others (1983) argued that the middle Cretaceous (100 Ma) experienced atmospheric CO_2 levels far higher than at present. By validating the longstanding greenhouse hypothesis for the warm Cretaceous, the geochemical-cycle paradigm expanded the reach of uniformitarian principles in geoscience (Lyell, 1837).

GEOCARB geochemical-cycle models are successors to the BLAG model that eschewed the explicit integration of the Urey reactions in favor of computing a series of steady-state carbon-flux balances through the Phanerozoic (Berner, 2004). The justification for the GEOCARB approach is similar to using a 1-D radiation balance to estimate the long-term effect of greenhouse gasses. Just as the heat capacity of Earth's surface is too small to sustain long-term imbalances in radiation through the atmosphere, the total mass of carbon in Earth's atmosphere, biosphere and ocean is too small to sustain long-term imbalances in global carbon fluxes. Just as temperature rises or falls to achieve a radiation balance with a particular mix of greenhouse gasses, the GEOCARB models allow the CO_2 concentration to rise and fall to balance carbon fluxes associated with rock weathering, organic carbon burial/exhumation, and degassing. Successive versions of the GEOCARB model versions have utilized improved proxies for geologic processes and increased the model's sophistication. Berner (1991) incorporated $\delta^{13}C$ as a proxy for carbon burial. Berner (1994) added strontium isotopes as a proxy for chemical weathering. Berner and Kothavala (2001) distinguished the weathering impact of angiosperms and gymnosperms. Berner (2001, 2006a) incorporated sulfur isotopes as a constraint on atmospheric O_2 levels. Most recently, Berner (2006b, 2008, 2009) applied proxies to distinguish between "volcanic" and "granitic" weathering in the updated GEOCARB-SULF model, to exploit their differing weathering susceptibilities.

Through two decades of refinement, the predictions of the GEOCARB family of geochemical models have shown robust associations between the history of Earth's climate, tectonics and biota, reflecting a variety of causal relationships (Berner, 2004). High CO_2 in the early Paleozoic compensates for a weaker coeval solar constant. The onset of glacial conditions in the late Paleozoic is associated with the rise of vascular plants and their enhancement of CO_2-consumption via silicate weathering. Mesozoic warmth is associated with increased degassing associated with more-vigorous tectonics, and weaker weathering due to less continental relief. No single geologic process dominates Phanerozoic climate history. Rather, a combination of processes acted over time to fluctuate greenhouse-gas concentrations, and helped to determine the long-term history of Earth climate. The GEOCARB models cannot be used directly to predict the ΔT_{2x} that today's generation of carbon-emitters should expect, because the carbon-flux balance is a long-term (>1 My) estimate of environmental processes. Nevertheless, the GEOCARB models validate the notion that anthropogenic CO_2 emissions will cause global warming and related climate changes.

Alternate models to the GEOCARB model-family exist both as global-average algorithms (Wallmann, 2001; Bergman and others, 2004; Arvidson and others, 2006), and as models that allow geographical variation in weathering processes and other feedbacks (Godderis and others, 2008, 2009). Experiments similar to those reported in this paper could be tried with alternate models, but parameterizations and feedbacks common to long-term carbon-cycle models suggest that our estimates of ΔT_{2x} from GEOCARBSULF will be representative. However, the use of a geographically-dependent carbon-cycle model for a well-documented interval of Earth history (for example, Godderis and others, 2008) might narrow the acceptable range of ΔT_{2x} in a particular geologic context, and reveal tradeoffs between environmental processes that are specific to the era studied.

Royer and others (2007) rewrote the original BASIC computer code for GEOCARB-SULF (Berner, 2006a) into FORTRAN (copy available at http://jparkcodes.blogspot.com/) in order to vary systematically five parameters whose value is imprecise during the full Phanerozoic (Berner, 2004). The first parameter was the main target of the study, the climate sensitivity ΔT_{2x}, crucial in creating the negative weathering feedback in an enhanced-greenhouse Earth. The parameter *ACT* is the activation energy for the dissolution of primary Ca- and Mg-silicates in continental interiors (for example, Dessert and others, 2001). The parameter *FERT* specifies the fraction of land-plant growth that responds to changes in atmospheric CO_2 concentration. The parameters *LIFE* and *GYM* scale the weathering efficiency of, respectively, an algal/bryophytic land biosphere (570-380 Ma) and a gymnosperm-dominated land biosphere (350-130 Ma), to present-day angiosperm-dominated values. As an example, *GYM* = 1 equates the weathering efficiency of gymnosperms and angiosperms. Weathering efficiency during 380 to 350 Ma is interpolated in time between the bryophytic and gymnosperm values. Weathering efficiency during 130 to 80 Ma is interpolated in time between the gymnosperm and angiosperm values. The effects of these parameters in GEOCARBSULF trade off with each other. The *GYM* and *LIFE* parameters modulate the effects of plant-assisted weathering at different intervals of the Phanerozoic, while *ACT* and *FERT* affect weathering at all times. There are many other parameters in GEOCARBSULF that affect its predictions of CO_2 through the Phanerozoic, such as the weatherable area of continents through time. In the Discussion we investigate this issue further.

Royer and others (2007) used the version of GEOCARBSULF documented by Berner (2004, 2006a). Berner (2006b, 2008, 2009) improved the model's realism by distinguishing between volcanic and plutonic Ca- and Mg-silicate weathering. Because volcanic rocks weather more readily than plutonic rocks (Meybeck, 1987) and contribute an estimated 30 to 35 percent of total silicate weathering (Dessert and others, 2003), this reformulation strengthens the weathering feedback in GEOCARBSULF significantly, and serves as one motivation for this study. We use the parameter NV = 0.15 to scale the contribution of volcanic, principally basaltic, weathering to the strontium isotope budget (Berner, 2006b). Basalts weather 1.5–3 times as quickly as granites (Meybeck, 1987; Taylor and others, 1999; Taylor, ms, 2000), but their net consumption of CO_2 is further boosted by their greater proportion of Ca and Mg (Taylor and others, 1999; Taylor, ms, 2000). We therefore set the ratio of volcanic and non-volcanic CO_2-consumption rates VNV = 4, twice the value assumed by Berner (2006b).

PROXY-CO_2 DATA AND BAYESIAN MODELING

The qualitative agreement of GEOCARB models with Phanerozoic climate history can be made quantitative by fitting the model to independent estimates of past atmospheric CO_2 levels (Royer and others, 2007; Fletcher and others, 2008). The proxy data for past CO_2 levels include the $\delta^{13}C$ of phytoplankton (Stott, 1992; Freeman and Hayes, 1992; Pagani and others, 1999a, 1999b, 2005), the stomatal density/index of fossil plant leaves (Van der Burgh and others, 1993; Beerling and others, 1998; McElwain, 1998; McElwain and others, 1999; Chen and others, 2001; Royer and others, 2001; Beerling, 2002; Beerling and others, 2002; Beerling and Royer, 2002; Greenwood and others, 2003; Roth-Nebelsick and Konrad, 2003; Haworth and others, 2005; Sun and others, 2007; Kürschner and others, 2008; Retallack, 2009b; Beerling and others, 2009; Passalia, 2009; Quan and others, 2009; Yan and others, 2009; Barclay and others, 2010; Doria and others, 2011), the fractionation of boron isotopes (Pearson and others, 2009), boron/calcium ratios (Tripati and others, 2009), $\delta^{13}C$ of liverwort fossils (Fletcher and others, 2008), and $\delta^{13}C$ of carbonate concretions in paleosols (Suchecki and others, 1988; Platt, 1989; Cerling, 1991, 1992; Koch and others, 1992; Muchez and others, 1993; Sinha and Stott, 1994; Andrews and others, 1995; Ghosh and others, 1995, 2001, 2005; Mora and others, 1996; Ekart and others, 1999; Lee and Hisada, 1999; Lee, 1999; Driese and others, 2000; Cox and others, 2001; Royer and others, 2001; Tanner and others, 2001; Robinson and others, 2002; Nordt and others, 2002, 2003; Tabor and others, 2004; Prochnow and others, 2006; Montañez and others, 2007; Cleveland and others, 2008; Retallack, 2009b; Breecker and others, 2009, 2010; Royer, 2010).

Proxy data for CO_2 suffers considerable scatter, but the sensitivity of global-average temperatures to CO_2 is logarithmic. The variation of CO_2 over the Phanerozoic is larger than the scatter of coeval proxy-CO_2 estimates, and improvements in the interpretation of proxy data can reduce the scatter. Beerling and others (2009) recalibrated the non-linear relationship between leaf-stomata density and CO_2 concentration. In soils, the $\delta^{13}C$ of pedogenic carbonates reflects a mixture of ambient atmospheric CO_2 and ^{12}C-dominated CO_2 respired by plants and soil-dwelling microbes (Cerling, 1991). Breecker and others (2009) argued from field data that $CaCO_3$ concretions in soils accumulate preferentially

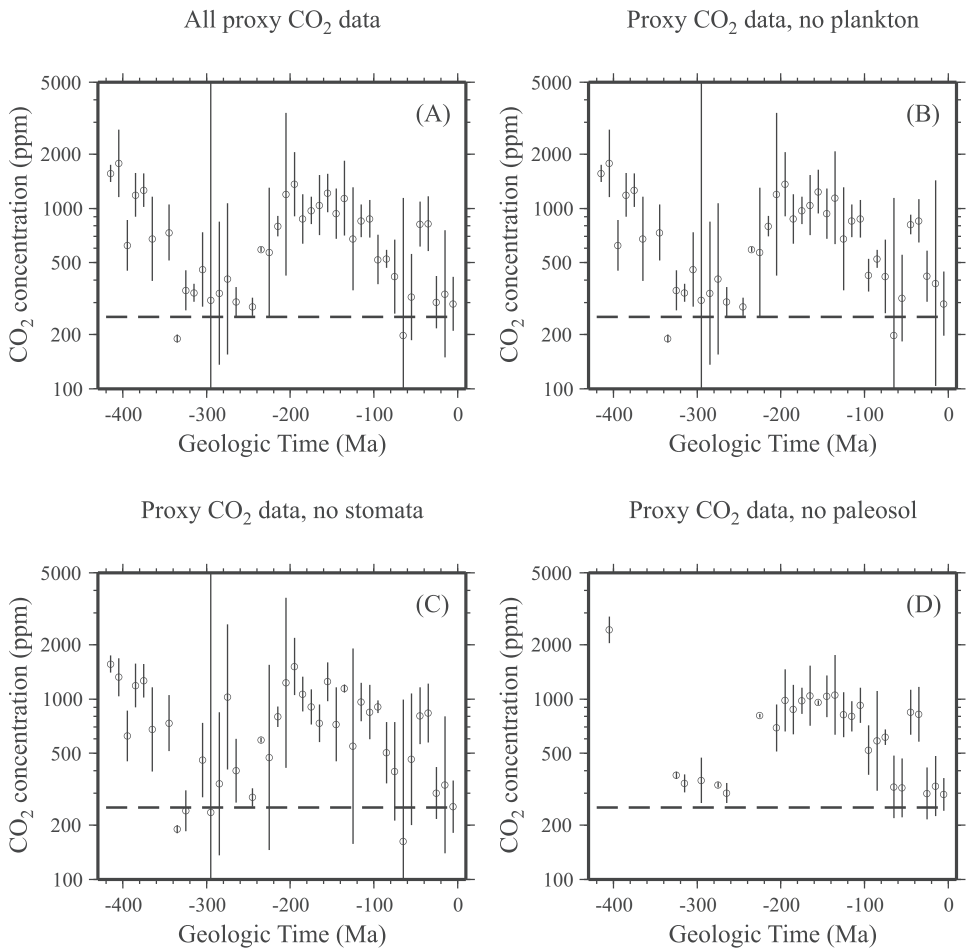

Fig. 1. Proxy-CO_2 data used in this study, expressed in 10-My moving averages centered on 5 Ma, 15 Ma, 25 Ma, *et cetera*. The baseline average Pleistocene CO_2-concentration (250 ppm) is plotted as a horizontal reference line. (A) All sources of proxy data are included (635 data); (B) CO_2-proxies based on phytoplankton fossils are omitted (451 data); (C) CO_2-proxies based on fossil leaf stomata are omitted (438 data); (D) CO_2-proxies based on paleosols are omitted (420 data).

outside the yearly growing season, when the light-isotope soil-derived CO_2 is less abundant. As a result, a lower atmospheric CO_2 concentration is necessary to explain the intermediate $\delta^{13}C$ values observed in paleosol carbonates. The recalibrated CO_2 estimates from paleosol carbonates bring them more in agreement with other CO_2 proxies (Royer, 2010), and suggest that past enhanced-greenhouse climate intervals, for example the Mesozoic, experienced CO_2 levels similar to those projected for 2100 AD (Breecker and others, 2010). Combined with age corrections according to Gradstein and others (2004), these adjustments to proxy-based estimates of Phanerozoic CO_2 levels are significant, another motivation for an update to the GEOCARB-based climate sensitivity study of Royer and others (2007).

We assembled a set of 635 proxy-CO_2 data for past 420 My of the Phanerozoic, based on the data sources and recalibrations listed above (fig. 1). For each datum we either used reported standard deviations, determined upper and lower 1-σ bounds on

CO_2-concentration based on related proxy data, or estimated sensitivity ranges from varying parameters in the formulas that relate proxy observations to atmospheric CO_2 concentration. We averaged the data in 10-My windows centered on 5 Ma, 15 Ma, 25 Ma, *et cetera,* using a weighting scheme based on logarithmic data uncertainties σ_i. Only one 10-My interval since 420 Ma lacks data, leading to N = 41 values for fitting with the GEOCARBSULF model. Because the climatic influence of atmospheric CO_2 depends on $\log(pCO_2)$, we averaged the logarithms of the data in the *k*th 10-My interval:

$$(pCO_2)_k^{avg} = \exp\left(\left(\sum_i \left(\frac{\log(pCO_2)_i}{\sigma_i^2}\right)\right) \Bigg/ \left(\sum_i 1/\sigma_i^2\right)\right) \quad (1)$$

where the weighting factor is computed from the estimated upper bound of the estimated uncertainty interval

$$\sigma_i = \log\left(\frac{(pCO_2)_i^{upper}}{(pCO_2)_i}\right) \quad (2)$$

For the uncertainty σ_k^{avg} of $\log(pCO_2)_{avg}$, we use the sample variance of $\log(pCO_2)$-proxy data in 10-My intervals. For intervals with $K \geq 2$ data points,

$$\sigma_k^{avg} = \sqrt{\sum_i \frac{(\log((pCO_2)_i/(pCO_2)_k^{avg}))^2}{(K-1)}} \quad (3)$$

and $\sigma_k^{avg} = \sigma_i$ if there is only K = 1 data point in the 10-My interval. The sample variance is more conservative than the standard variance-of-the-mean estimate $\hat{\sigma}^2 = 1\Big/\left(\sum_i 1/\sigma_i^2\right)$. Neither the CO_2-proxy data nor the 10-My averages $(pCO_2)_k^{avg}$ are Gaussian random variables, but their logarithms better approximate Gaussian statistics. We use terminology drawn from Gaussian statistics, such as data-fitting within uncertainty bounds and χ^2 values:

$$\chi^2 = \sum_k \frac{\left(\log\left(\frac{(pCO_2)_k^{avg}}{(pCO_2)_k^{predicted}}\right)\right)^2}{(\sigma_k^{avg})^2} \quad (4)$$

The colloquial metric for this expression is the root-mean-square (rms) data misfit in units of σ_k^{avg} from (3). For Gaussian statistics, a "one-sigma" rms misfit is the desirable situation, because it allows the data to scatter about model predictions in a manner consistent with the observational uncertainties. A rms misfit $<1\sigma$ risks fitting noise as well as signal. A rms misfit $> 1\sigma$ suggests that the model has shortcomings.

The complement to χ^2 misfit is the variance reduction, the fraction of the total proxy-CO_2 data variance that GEOCARBSULF explains (fig. 2). To calculate data variance, one must define a baseline value that a dataset departs from. For this application we define the baseline as uniform pre-industrial/Late-Pleistocene atmospheric CO_2 concentrations for all time. In the GEOCARBSULF computer code, pre-industrial/late-Pleistocene CO_2 is 250 ppm, the estimated average value over the past million years (Berner, 2006a). Departure from the baseline CO_2 value is measured in logarithmic units, in terms of σ_k^{avg} as defined by (3).

Bayesian probability density functions, also known as empirical PDFs, quantify the probability that a particular value of a model-parameter leads to model-predictions

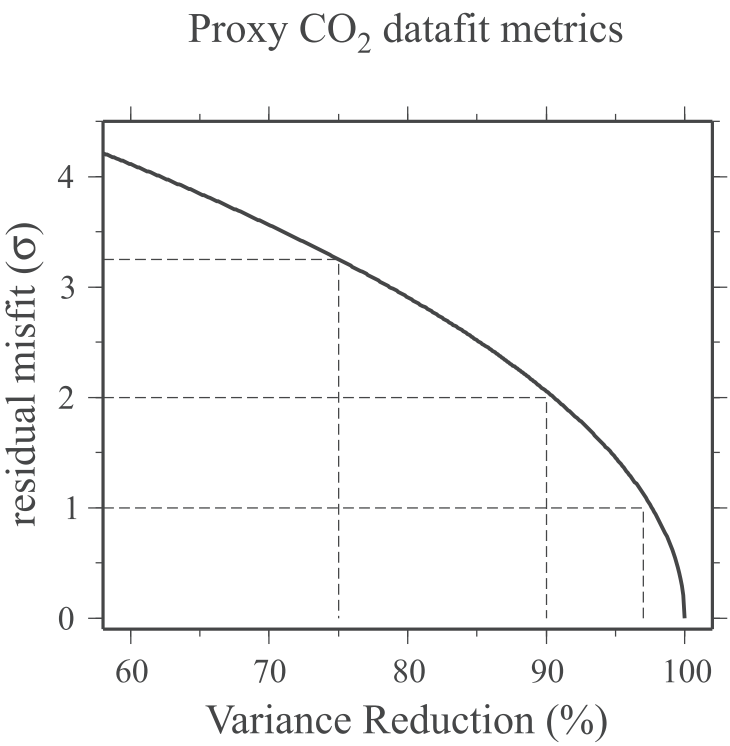

Fig. 2. Datafit metrics for proxy-CO_2 data. The total data variance is based on standard deviation σ, from the Pleistocene average (250 ppm). The variance of the 10-My moving-average proxy-CO_2 data corresponds to 6.5σ rms misfit. Three approximate reference points are marked by dashed lines: 75% data variation and 3.25-σ data misfit, 90% data variance fit and 2-σ data misfit, and 97% data variation and 1-σ data misfit.

that are consistent with a set of hypotheses and/or observations. A simple example of this concept comes from introductory probability theory. If a person throws two dice, each die can return an integer value from one to six with equal probability, but the probability of the combined total, from two through twelve, has a binomial probability that peaks at the number seven. Suppose we constrain the total number on the dice to be three. What is the probability for the numbers on one die? By noting the number of dice combinations that can result in a total of three, the probability for each die is 50 percent one, 50 percent two, and zero-probability for all other values. Our GEOCARBSULF modeling experiment is more complicated than a dice throw, but its principle is similar. If GEOCARBSULF is required to fit the proxy-CO_2 data within a particular tolerance, subject to plausible variations in the four parameters *FERT, LIFE, GYM* and *ACT*, what is the probability that ΔT_{2x} falls within a specified range? If all allowed values of the parameters *FERT, et cetera,* are assumed to be equally probable, similar to a dice throw, then the most-probable value of climate sensitivity ΔT_{2x} is the value that can fit the proxy-CO_2 data with the largest number of parameter combinations.

In an earlier example of our modeling strategy, Forest and others (2002) compared the output of a coupled dynamical atmosphere-ocean model with climate observations of the late 20th century, to determine which values of climate sensitivity replicated the gross features of historical climate (mean temperatures, trends) most robustly with respect to plausible variations of unknown physical parameters, such as ocean heat diffusivity and atmospheric aerosol radiation forcing. Royer and others

(2007) applied Bayesian PDFs to the climate sensitivity ΔT_{2x} in the GEOCARBSULF model, determining the probability that the carbon-cycle model could fit CO_2-proxy data within a chosen χ^2 misfit, within allowable ranges of the parameters $0.2 \leq FERT \leq 0.8$, values of $0.03 \leq ACT \leq 0.13$ corresponding to activation energies 20 to 83 kJoule/mole, $0.125 \leq LIFE \leq 0.5$, and $0.5 \leq GYM \leq 1.2$. GEOCARBSULF was run in an evenly-spaced grid search over these four parameter ranges, 10 values per parameter, as well as evenly-spaced climate-sensitivity values $0.6\ °C \leq \Delta T_{2x} \leq 10.4\ °C$. Each value of ΔT_{2x} was run with 10000 GEOCARBSULF simulations, and the number of simulations that fit data better than a chosen χ^2 misfit was tabulated. With suitable normalization of the success ratio for all tested values of ΔT_{2x}, a plot of success ratio versus climate sensitivity represents the Gaussian PDF. In practice, the choice of datafit affects the shape of the PDF. A too-stringent χ^2-misfit criterion for the proxy-CO_2 data causes the success ratio to vanish for some values of ΔT_{2x}. A too-loose χ^2-misfit criterion saturates the success ratio at values approaching unity, discriminating poorly between different ΔT_{2x} values. We test a small number of χ^2-misfit values to explore the robustness of the empirical PDF. The peak of the empirical PDF for climate sensitivity corresponds to the value of ΔT_{2x} for which the greatest number of other model-parameter combinations achieve or better a chosen χ^2-misfit value.

We replicate the computational strategy of Royer and others (2007) with a few changes. We sample ΔT_{2x} nonuniformly, exploiting the weak variation in GEOCARBSULF behavior at larger ΔT_{2x} values. We weight the model's success ratios with the local ΔT_{2x} spacing for proper normalization. Rather than focus exclusively on the empirical PDF for ΔT_{2x}, we explore model-parameter tradeoffs with another tactic employed by Forest and others (2002): by computing bivariate empirical PDFs from the success ratio of GEOCARBSULF at a 2-D grid of model-parameter choices. For instance, we evaluate GEOCARBSULF at a particular choice of ΔT_{2x} and *ACT* with 1000 model runs, corresponding to a gridsearch over the remaining three model parameters *FERT*, *GYM* and *LIFE*. The bivariate PDF for *ACT* and ΔT_{2x} can be obtained after normalizing a 2-D grid of success ratios. Finally, we extend the parameterization of Royer and others (2007) to allow independent climate sensitivities in geologic time invervals characterized by glacial and nonglacial conditions. Although no division of nonglacial and glacial climate periods lacks potential controversy, we chose the intervals 260 to 340 Ma and 0 to 40 Ma to be glacial for this study, consistent with Crowley (1998).

Empirical PDFs from a modeling study must be interpreted carefully. Bayesian probabilities are contingent on *a priori* assumptions that often are artificial. In this study, one *a priori* assumption is that the GEOCARBSULF parameters *FERT*, *ACT*, *GYM* and *LIFE* are equally probable at any value within their allowed intervals, but lie outside the interval with zero probability. If the probability distribution of a GEOCARBSULF parameter were known to be Gaussian about a most-likely value, this *a priori* parameter PDF would alter the estimated empirical PDF, perhaps significantly. Plots of the bivariate empirical PDFs can help identify which empirical PDFs are vulnerable to this effect.

CLIMATE SENSITIVITY AND PARAMETER TRADEOFFS

The revisions to the GEOCARBSULF model for volcanic-silicate weathering (Berner, 2006b, 2008, 2009) plus the expansion and recalibration of the proxy-CO_2 data set (Beerling and others, 2009; Breecker and others, 2009, 2010; Royer, 2010) leave the conclusions of Royer and others (2007) about the empirical PDF of ΔT_{2x} largely unchanged. Figure 3 plots the empirical PDF and cumulative distribution functions (integrals of the PDFs) for 75 percent, 80 percent and 85 percent variance reduction. The 85 percent variance-reduction curves correspond to model-parameter choices that misfit the data $<2.5\sigma$. The best misfit possible with our parameterization

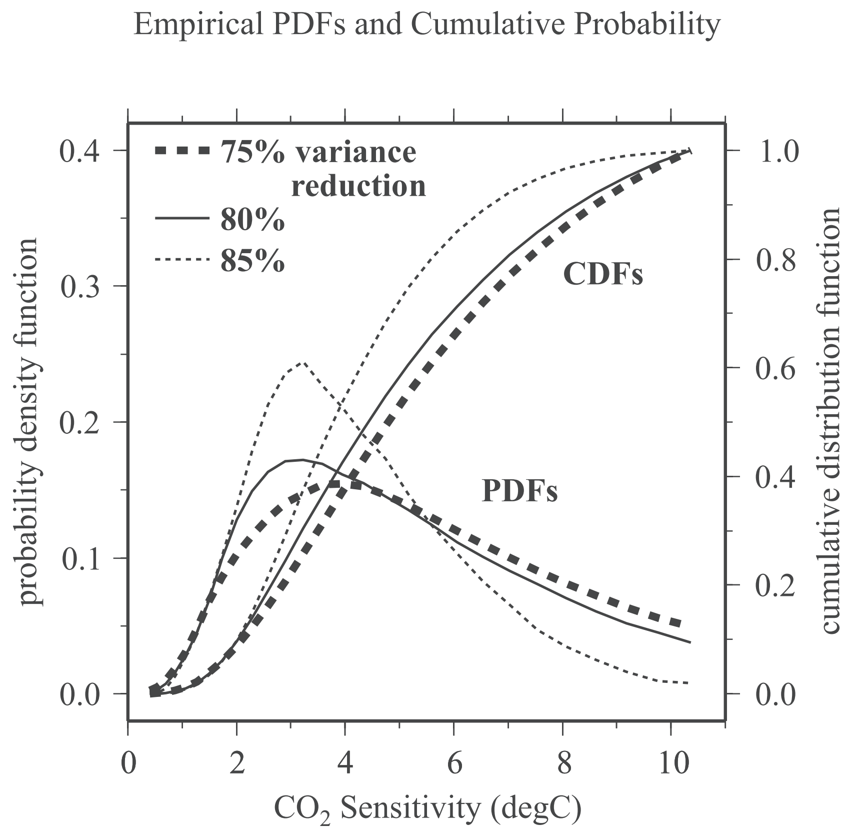

Fig. 3. Empirical probability density functions (PDFs) and cumulative distribution functions (CDFs) for the long-term climate sensitivity ΔT_{2x} of average Earth temperature to a doubling of atmospheric CO_2 concentration. A uniform Phanerozoic climate sensitivity ΔT_{2x} is assumed in this experiment. The empirical PDF is high where a larger number of combinations of the GEOCARBSULF parameters *LIFE*, *ACT*, *GYM* and *FERT* can achieve a specified level of variance reduction in the 10-My-averaged proxy-CO_2 data, relative to baseline Pleistocene values (fig. 1). The PDFs are normalized to unit-integral over $0° \geq \Delta T_{2x} \geq 10.4$ °C.

choices is 2.14σ, corresponding to 89 percent variance reduction. Variations in the PDF and CDF curves derive from the concentration of the best-fitting GEOCARBSULF model runs at the most-probable $\Delta T_{2x} = 3.2$ °C value. If greater misfit is allowed (75% variance reduction, all models with data misfit $<3.25\sigma$), the most-probable climate sensitivity shifts to higher $\Delta T_{2x} = 3.9$ °C. For all three choices of variance reduction, the climate sensitivity $\Delta T_{2x}>1.0$ °C with ~99 percent probability, $\Delta T_{2x}>1.5$ °C with ~95 percent probability, and $\Delta T_{2x}>2.0$ °C with ~90 percent probability. We confirm the conclusion of Royer and others (2007): the necessity for greenhouse-weathering feedbacks in Earth's long-term carbon cycle makes low values for Earth's long-term climate sensitivity ΔT_{2x} highly unlikely.

Bivariate empirical PDFs reveal interesting correlations within our GEOCARBSULF experiment (fig. 4). The sharpest feature in the joint PDFs of ΔT_{2x} with the other adjustable parameters is the peak probability found at (ΔT_{2x}, *GYM*) ≈ (2.8 °C, 0.9). Interpreting this PDF peak, GEOCARBSULF fits the proxy-CO_2 data most readily for 2.5 °C < ΔT_{2x} < 3.0 °C and gymnosperm weathering only slightly less efficient than angiosperm weathering. The PDF peak is slightly broader at higher ΔT_{2x} values, so that the univariate PDF for ΔT_{2x} peaks at a slightly higher value. It is interesting to note that

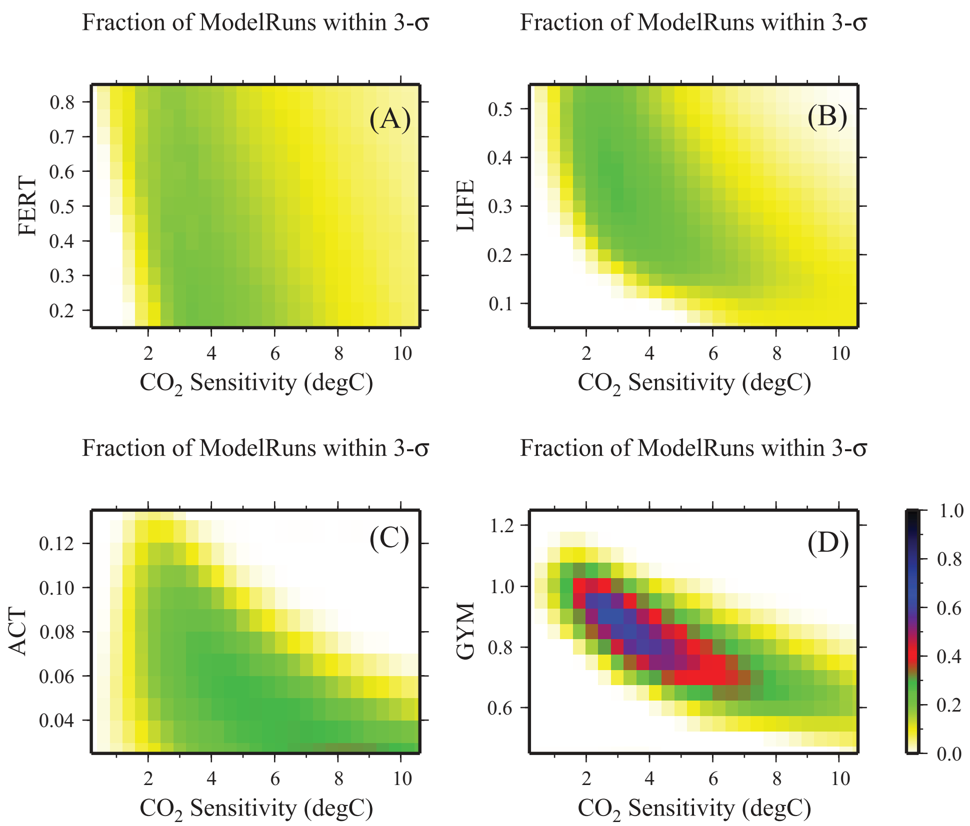

Fig. 4. Bivariate empirical PDFs of GEOCARBSULF parameters with long-term climate sensitivity ΔT_{2x}. A uniform Phanerozoic climate sensitivity ΔT_{2x} is assumed in this experiment. The PDFs are not unit-normalized, rather, the colors correspond to the fraction of chosen parameters combinations (1000 total cases at each point) for which GEOCARBSULF fits the 10My-averaged proxy-CO_2 data with rms misfit $\leq 3\sigma$. Bivariate PDFs plotted for ΔT_{2x} versus (A) CO_2fertilization fraction *FERT*, (B) relative weathering efficiency *LIFE* for the early Paleozoic liverwort/bryophyte terrestrial biosphere, (C) weathering activation-energy parameter *ACT*, and (D) relative weathering efficiency *GYM* for the Paleozoic-Mesozoic gymnosperm terrestrial biosphere.

peak probability at higher climate sensitivities ΔT_{2x} occurs for smaller *GYM*, that is, less-efficient gymnosperm weathering. A far weaker trend can be seen in the bivariate PDF of ΔT_{2x} with *LIFE*, which peaks at bryophyte/liverwort weathering 30 to 40 percent as efficient as angiosperm weathering. Weak variation in the bivariate PDF for ΔT_{2x} and *FERT* suggests that our GEOCARBSULF experiment shows very little preference for particular values of *FERT*, the effective fraction of land plants whose growth is fertilized by higher CO_2 levels.

The bivariate PDF between ΔT_{2x} and the activation-energy parameter *ACT* shows a clear inverse proportionality (fig. 4). This trend implies that, as ΔT_{2x} increases, better datafits are obtained with smaller *ACT*. Berner (2004) relates the parameter $Z = ACT$ to the activation energy ΔE of weathering via

$$Z = ACT = \frac{\Delta E}{RTT_o} \tag{5a}$$

where R = 8.314472 J/(mol-°K) is the gas constant, T is the ambient temperature (in °K), and T_o=288 °K is the reference-mean global temperature. Weathering reaction rates J in the model are a function of global-average temperature T

$$J/J_o = \exp(Z(T - T_o)) \tag{5b}$$

where J_o is the reaction rate at reference temperature T_o. The parameter *ACT* scales the temperature sensitivity of the silicate weathering process (Berner and Kothavala, 2001), so an inverse relationship with ΔT_{2x} is expected. Two additional features are notable for the ΔT_{2x}-*ACT* PDF. First, the PDF lacks a strong preference for *ACT* if ΔT_{2x}~3.0 °C. Second, the low values of *ACT* that pair well with high climate sensitivity (ΔT_{2x}>4 °C) are lower than suggested by most laboratory and field studies. The lowest values for ΔE in Table 2.2 of Berner (2004) are roughly 42 kJ/mol, corresponding to *ACT* = 0.06. Activation energies for granitic rocks and terranes typically correspond to the upper range of *ACT*, and fit the proxy-CO_2 data less well when coupled with higher values of ΔT_{2x}. Lower activation energies have been found for volcanic glasses in laboratory studies (Gislason and Oelkers, 2003) and field studies in basaltic river catchments in Iceland (Gislason and others, 2009), so the full range of *ACT* in our experiment covers the range of field observations.

If we apply a nonuniform prior distribution $P(ACT)$ to the $0.03 = ACT_{min} \leq ACT \leq ACT_{max} = 0.13$ interval that expresses an interpretation of published data for the global activation energy ΔE, the Bayesian empirical PDF for ΔT_{2x} will change. One such prior for *ACT* could be

$$P(ACT) = \frac{\left(0.5 + \sin^2\left(\frac{\pi(ACT - ACT_{min})}{2(ACT_{max} - ACT_{min})}\right)\right)}{(ACT_{max} - ACT_{min})} \tag{6}$$

for which $P(ACT_{max}) = 3P(ACT_{min})$. Using (6) in the GEOCARBSULF computations causes the empirical PDF for ΔT_{2x} to decline more steeply at ΔT_{2x}>4 °C (fig. 5). Many estimation studies for climate sensitivity are heavy-tailed at large ΔT_{2x} values (Knutti and Hegerl, 2008), but other considerations could dampen these probabilites. Urban and Keller (2009) cite a case where climate-process correlations dampen the PDF tail. In our study the argument for dampening the high-ΔT_{2x} tail of the PDF rests on the presumption that low values of *ACT* are less probable.

Hansen and others (2008), Pagani and others (2010) and others have hypothesized that long-term climate sensitivity is greater in glacial intervals of Earth history, due to the slow amplification of short-term greenhouse warming by ice sheets. In GEOCARBSULF modeling we are free to specify a time-dependent climate sensitivity ΔT_{2x}, and use its evolving value to balance carbon fluxes as GEOCARBSULF marches through the Phanerozoic. In this study, we define a glacial $\Delta T_{2x}^{(g)} = GLAC \times \Delta T_{2x}$ with a coefficient *GLAC* that allows independent climate sensitivity in glacial and non-glacial intervals. The glacial intervals are taken to be 0 to 40 Ma, based on the onset of Cenozoic glaciation of Antarctica at 34 Ma (Zachos and others, 1999; DeConto and Pollard, 2003), and 260 to 340 Ma, based on compilations of Paleozoic glacial deposition (Fielding and others, 2008; see also Crowley, 1998). In order to avoid adding a sixth dimension to the parameter gridsearch, we fixed *FERT* = 0.5 and allowed *GLAC* to vary over 10 values, spaced logarithmically from 0.5 to 4.0. The carbon-cycle model GEOCARBSULF favored parameter choices that included substantial glacial amplification of climate sensitivity. More than 40 percent of GEOCARBSULF runs fit the proxy-CO_2 data within 3σ rms misfit if the non-glacial 3.5 °C < ΔT_{2x} < 5.5 °C and *GLAC* > 2 (fig. 6A).

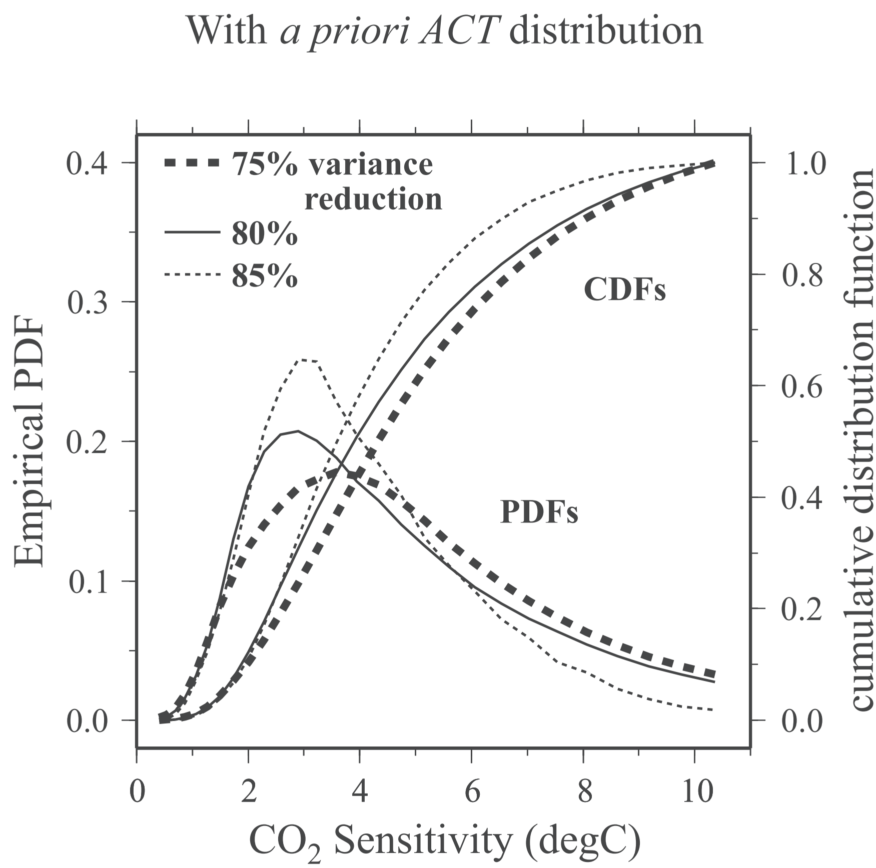

Fig. 5. Empirical probability density functions (PDFs) and cumulative distribution functions (CDFs) for the long-term climate sensitivity ΔT_{2x} of average Earth temperature to a doubling of atmospheric CO_2 concentration. These PDFs use an *a priori* PDF (6) for the activation-energy parameter *ACT* that downweights *ACT*<0.08 values, effectively decreasing the PDF at $\Delta T_{2x} > 4$ °C. A uniform Phanerozoic climate sensitivity ΔT_{2x} is assumed in this experiment. The PDFs are normalized to unit-integral over $0° \geq \Delta T_{2x} \geq 10.4$ °C.

Although the GEOCARBSULF carbon-cycle model does not incorporate glacial processes in an explicit manner, the model fits data most readily if its glacial climate sensitivity is much greater than its nonglacial climate sensitivity. The model does not prefer lower values of nonglacial ΔT_{2x} than for the uniform-sensitivity case. In fact, the empirical PDF for non-glacial climate sensitivity ΔT_{2x} is largely unchanged if we set *GLAC* = 2 for model runs with ≤85 percent variance reduction (fig. 7, compare with fig. 3). The looser datafit constraints, for ≤80 percent and ≤75 percent variance reduction, lead to empirical PDFs with non-glacial sensitivity maxima at higher values, near 4 °C. Because *GLAC* = 2 specifies that glacial climate sensitivity is twice that of the non-glacial climate, PDF peaks at ΔT_{2x} = 3°–4 °C imply that most-probable glacial $\Delta T_{2x}^{(g)}$ = 6°–8 °C. It seems clear that GEOCARBSULF has little difficulty reconciling the proxy-CO_2 data set with glacial climate sensitivities $\Delta T_{2x}^{(g)}$ in the 7.1° to 9.6 °C range inferred by Pagani and others (2010), which was based on comparing the present-day with the Pliocene (sampled at 3.3-4.2 Ma). The above statement gains force after perusal of figure 6 shows that *GLAC* = 2 might underestimate the most-probable

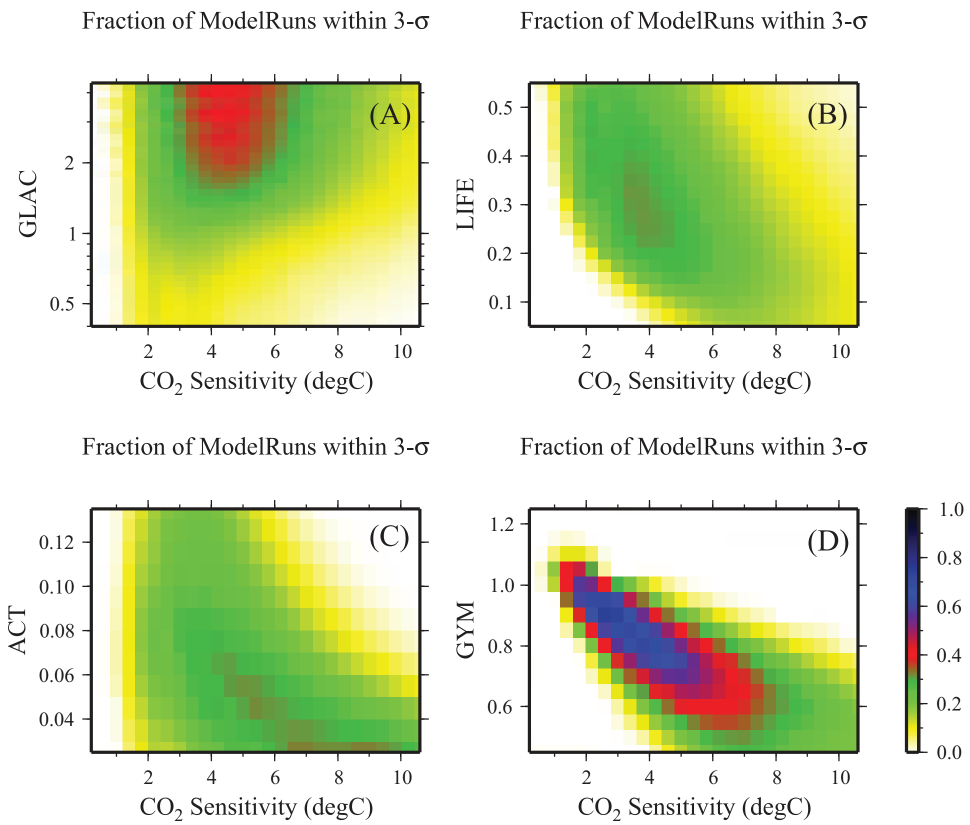

Fig. 6. Bivariate empirical PDFs of GEOCARBSULF parameters with long-term climate sensitivity $\Delta T_{2x}^{(g)}$. Long-term glacial climate sensitivity $\Delta T_{2x}^{(g)} = GLAC \times \Delta T_{2x}$ is assumed to be proportional to long-term nonglacial climate sensitivity ΔT_{2x}, with fixed *FERT* = 0.5. The PDFs are not unit-normalized, rather, the colors correspond to the fraction of chosen parameters combinations (1000 total cases at each point) for which GEOCARBSULF fits the 10-My-averaged proxy-CO_2 data with rms misfit $\leq 3\sigma$. Bivariate PDFs plotted for ΔT_{2x} versus (A) glacial amplification *GLAC*, (B) relative weathering efficiency *LIFE* for the early Paleozoic liverwort/bryophyte terrestrial biosphere, (C) weathering activation-energy parameter *ACT*, and (D) relative weathering efficiency *GYM* for the Paleozoic-Mesozoic gymnosperm terrestrial biosphere.

glacial amplification. Using the scaling factor *GLAC* = 2, we can define lower bounds on climate sensitivity in the glacial intervals of Earth history. For all choices of misfit thresholds, the glacial climate sensitivity $\Delta T_{2x}^{(g)} > 2.0$ °C with ~99 percent probability, $\Delta T_{2x}^{(g)} > 3.4$ °C with ~95 percent probability, and $\Delta T_{2x}^{(g)} > 4.4$ °C with ~90 percent probability.

For glacial amplification *GLAC* = 2, the maxima of the bivariate empirical PDFs move closer to the center of their assumed parameter ranges (fig. 8). The darker colors in the plots demonstrate that glacial amplification allows a larger number of GEOCARBSULF parameter choices to fit the data within a given misfit threshold (rms misfit $< 3\sigma$ in figs. 4, 6 and 8). The smallest possible rms misfit over all parameter choices (~2.15σ) does not drop for *GLAC* = 2, however. Figure 8 shows local maxima of the bivariate PDFs found by pairing non-glacial $\Delta T_{2x} = 4$ °C (glacial $\Delta T_{2x}^{(g)} = 8$ °C) with *ACT* = 0.10, *LIFE* = 0.3, *GYM* = 0.8 and a wide range of *FERT* values. If a more stringent data-misfit criterion were applied, the bivariate PDF peaks would shift to slightly lower values, closer to non-glacial $\Delta T_{2x} = 3$ °C (glacial $\Delta T_{2x}^{(g)} = 6$ °C).

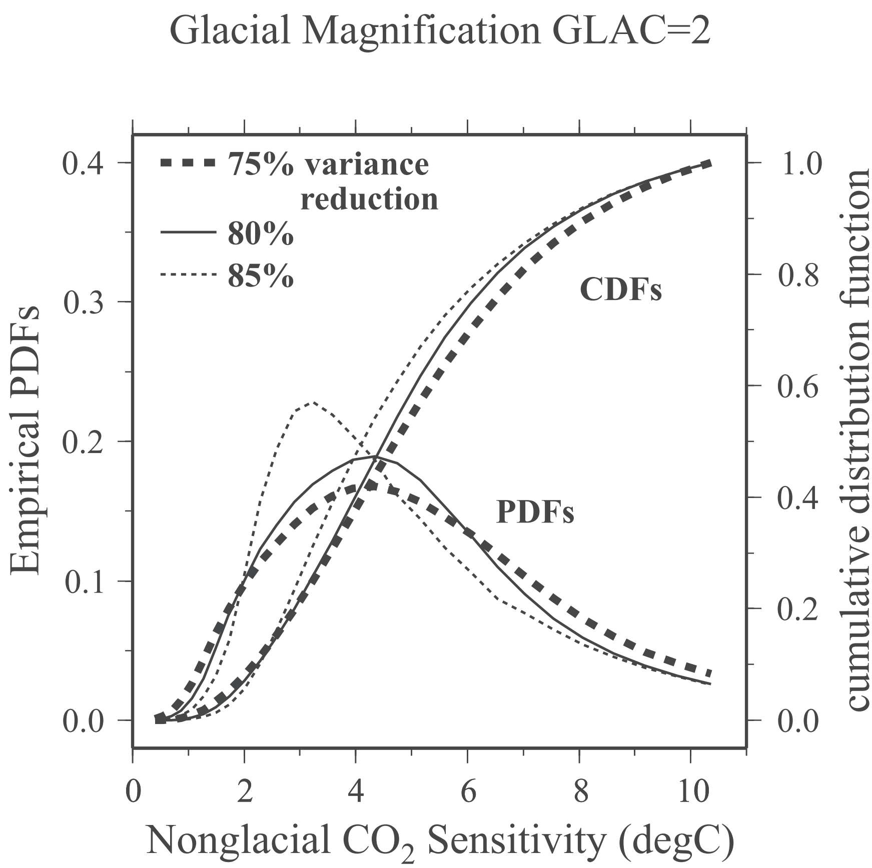

Fig. 7. Empirical probability density functions (PDFs) and cumulative distribution functions (CDFs) for the long-term nonglacial climate sensitivity ΔT_{2x} of average Earth temperature to a doubling of atmospheric CO_2 concentration. These PDFs are for *GLAC* = 2, meaning that glacial climate sensitivity $\Delta T_{2x}^{(g)} = 2\times\Delta T_{2x}$. In particular, the peak PDF near nonglacial ΔT_{2x} = 3 °C is paired with glacial climate sensitivity $\Delta T_{2x}^{(g)}$ = 6 °C. These PDFs use an *a priori* PDF (6) for the activation-energy parameter *LIFE* that downweights $ACT < 0.08$ values. The PDFs are normalized to unit-integral over $0° \geq \Delta T_{2x} \geq 10.4$ °C.

DATA FITTING AND DISCUSSION

The GEOCARBSULF model explains >85 percent of the proxy-CO_2 data variance ($\leq$2.52σ rms misfit) with a significant population of parameter choices, strong evidence that the model represents correctly many important earth-system processes. No choice of parameters in our experiment causes GEOCARBSULF to fit the data with a 1σ rms data misfit, suggesting that some earth-system processes are inadequately represented or else neglected entirely. Comparison of the proxy-CO_2 data with an ensemble of model CO_2-predictions (fig. 9) reveals that there are at least two well-sampled Phanerozoic intervals where GEOCARBSULF underpredicts the proxy-CO_2 data: 150 to 200 Ma and 30 to 50 Ma, coinciding roughly with the Jurassic period and the Eocene epoch. Significant mismatches also occur near the start and end of the late-Paleozoic glacial period (245 Ma and 355 Ma).

The persistent nature of the data-model misfits in figure 9 argues that the adjustable parameters in our GEOCARBSULF experiment do not have sufficient time resolution to nudge the model into better agreement with proxy-CO_2 data in time

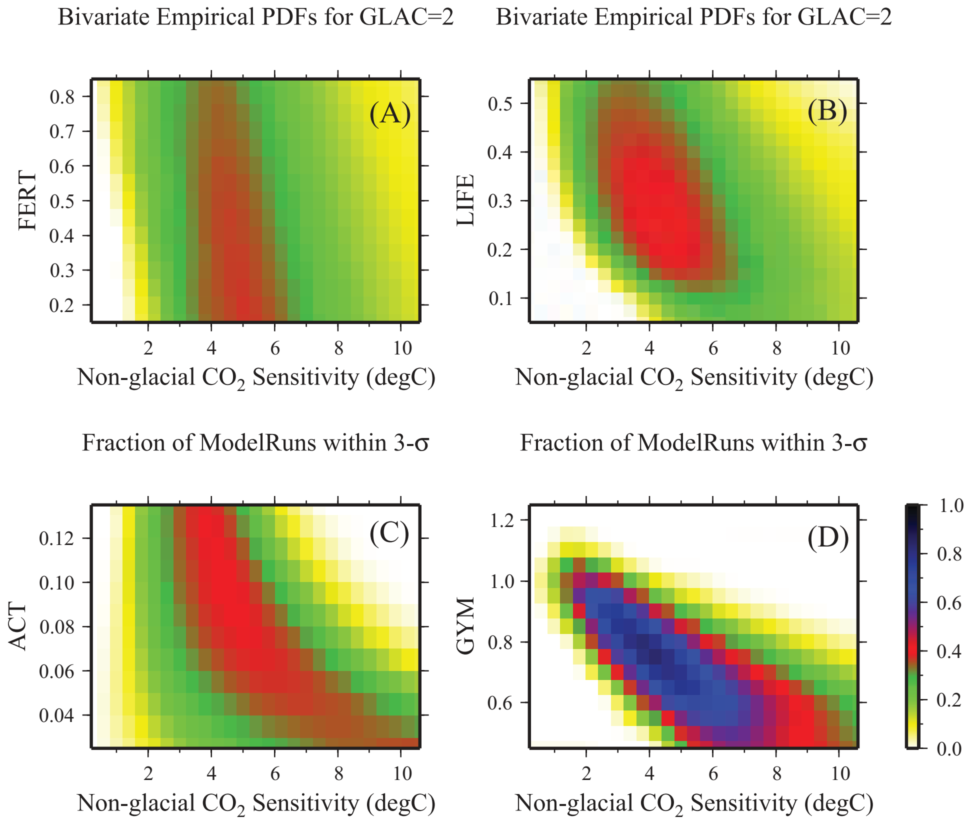

Fig. 8. Bivariate empirical PDFs of GEOCARBSULF parameters with long-term nonglacial climate sensitivity ΔT_{2x}. These PDFs are for *GLAC* = 2, meaning that long-term glacial climate sensitivity $\Delta T_{2x}^{(g)} = 2\times\Delta T_{2x}$. The PDFs are not unit-normalized, rather, the colors correspond to the fraction of chosen parameters combinations (1000 total cases at each point) for which GEOCARBSULF fits the 10-My-averaged proxy-CO_2 data with rms misfit $\leq$3-σ. Bivariate PDFs plotted for ΔT_{2x} versus (A) CO_2-fertilization fraction *FERT*, (B) relative weathering efficiency *LIFE* for the early Paleozoic liverwort/bryophyte terrestrial biosphere, (C) weathering activation-energy parameter *ACT*, and (D) relative weathering efficiency *GYM* for the Paleozoic-Mesozoic gymnosperm terrestrial biosphere.

windows of 50 My or less. There could be shortcomings in other parameterizations within GEOCARBSULF. Barring short-run mis-interpretations of strontium- and carbon-isotope data as global indicators of weathering and organic-carbon burial, respectively, a likely contender for adjustment is the weatherable continental area $f_A(T)$ on Earth as a function of time (Berner, 2004). GEOCARBSULF takes the weatherable land area to be equal to the total continental land area, obtained via plate-tectonic reconstructions, but this identification may be too simple. Cool climate within high-latitude continents may retard chemical weathering, for example.

Godderis and others (2008, 2009) argue that low-relief tropical continents develop a thick profile of weathered silicate that inhibits further weathering. As evidence, Godderis and others (2008) cites measurements of tropical watersheds, which are starved of dissolved weathering reaction-products relative to river catchments in temperate zones. Weak tropical weathering has the potential to raise atmospheric CO_2 concentration, because ever-warmer climates are necessary to boost chemical weathering in other latitude bands. After parameterizing this behavior into the geographical

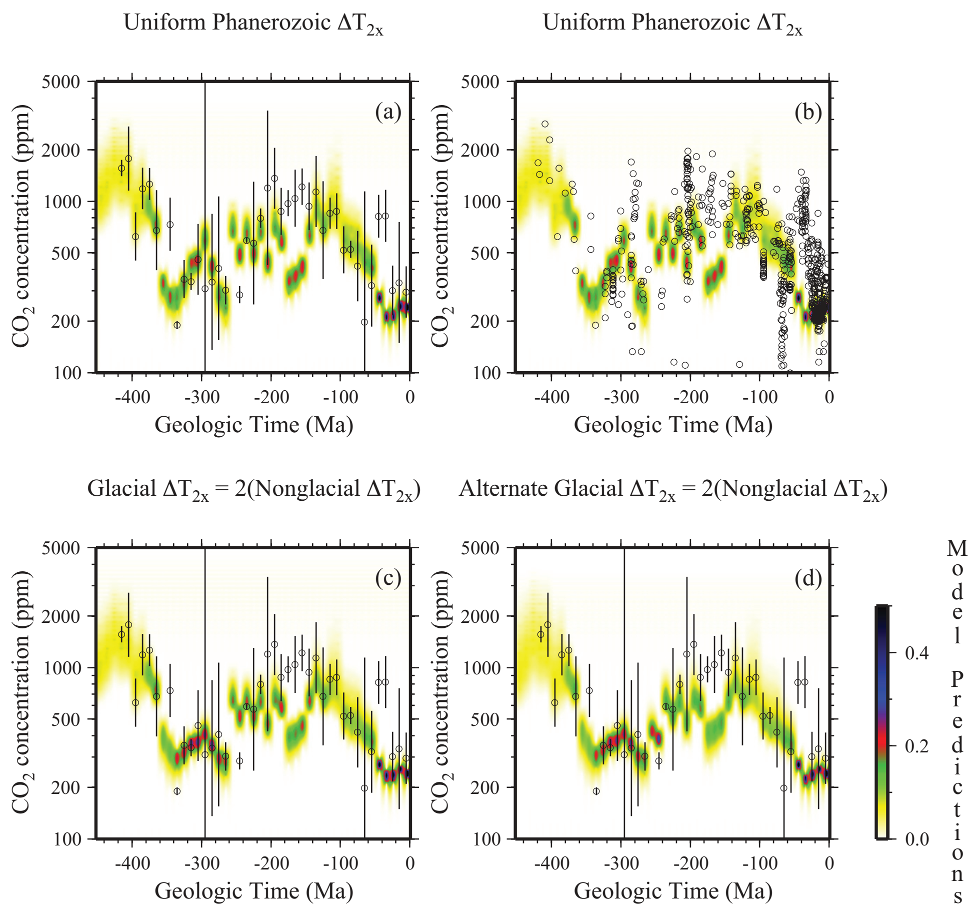

Fig. 9. Proxy-CO_2 data versus GEOCARBSULF model predictions for all parameter combinations *FERT*, *LIFE*, *GYM*, *ACT* and ΔT_{2x} that fit 10-My-averaged data with $\geq$ 85% data variance (rms data misfit $\leq$2.52-σ). The colors correspond to the density of CO_2 ppm values predicted by GEOCARBSULF, spaced at 1-My intervals in the Phanerozoic: (A) interval-averaged proxy-CO_2 data versus best-fit GEOCARBSULF results for a uniform Phanerozoic climate sensitivity ΔT_{2x}, (B) individual proxy-CO_2 data versus best-fit model results for a uniform Phanerozoic climate sensitivity ΔT_{2x}, recalibrated according to Breecker and others (2009, 2010), Beerling and others (2009) and Gradstein and others (2004), (C) interval-averaged proxy-CO_2 data versus best-fit model results for a glacial climate sensitivity $\Delta T_{2x}^{(g)} = 2\times\Delta T_{2x}$ for 0–40 Ma and 260–340 Ma, (D) interval-averaged proxy-CO_2 data versus best-fit model results for a glacial climate sensitivity $\Delta T_{2x}^{(g)} = 2\times\Delta T_{2x}$ for 0–30 Ma and 240–340 Ma.

GEOCLIM carbon-cycle model for past Earth climates, Godderis and others (2008) find that an unusual preponderance of low-latitude, low-relief continents in their Early-Middle Jurassic continental reconstruction leads to a two-fold increase in modeled CO_2. The GEOCARBSULF-Jurassic mismatch is closer to a factor of three, but the sign of the effect is consistent with the Godderis and others (2008) conjecture.

The GEOCARBSULF-Eocene mismatch lacks a similar explanation at this time. The Eocene marks the climax of a 200-My geologic interval of globally-warm climate. Many researchers have sought clues in Eocene paleogeography, ocean circulation and sediments for causal factors behind the transition toward Cenozoic cooling and glaciation (Raymo and Ruddiman, 1992; Sloan and Rea, 1995; Lear and others, 2000; Zachos and others, 2001, 2008; DeConto and Pollard, 2003; Pearson and others, 2007;

Smith and others, 2009; Westerhold and Rohl, 2009). Although some earlier proxy-CO_2 data suggested an erratic decline in CO_2 concentrations from >2000 ppm to values near pre-industrial (Pearson and Palmer, 2000; Zachos and others, 2001), recent data from many sources consistently indicate concentrations throughout the Eocene >500 ppm, with averages near 1000 ppm (Greenwood and others, 2003; Pagani and others, 2005; Zachos and others, 2008; Pearson and others, 2009; Retallack, 2009a; Doria and others, 2011). Reconciling such values with the 34-Ma onset of Antarctic glaciation (Zachos and others, 1999) must be considered an interesting geologic paradox in need of further study.

The model GEOCARBSULF, with its 10-My-averaged carbon-flux balances, is a blunt tool for investigating the complexities of the transition from Earth's "greenhouse" to "icehouse" climate states during the Eocene epoch. For instance, Zachos and others (2008) note that the early Cenozoic is punctuated by several rapid environmental releases of $\delta^{13}C$-depleted carbon in hyperthermal events, whose re-adsorption into the Earth system is outside the mechanistic scope of GEOCARBSULF. Speculatively, climate factors independent of greenhouse gasses, such as ocean circulation changes (Lear and others, 2000; Zachos and others, 2001), may have chilled Antarctica enough to dampen silicate weathering there, thereby lifting CO_2 levels and warming the climate to weather enough silicate on the remaining land to balance the Eocene carbon cycle. The thermal isolation of Antarctica astride the South Pole is often cited as an important factor in the initiation of its ice sheet at the Eocene-Oligocene transition, but high-latitude cooling is evident long before this juncture. Pearson and others (2007) used $\delta^{18}O$ from microfossil tests to argue that tropical SST remained warm throughout the Eocene, while the high-latitude deep-water source gradually grew colder over the epoch. Liu and others (2009) document SST$\geq$20°C for late-Eocene sites $\leq$70° latitude, but the existence of coeval 4 °C (Zachos and others, 2001) to 10 °C (Pearson and others, 2007) bottom water suggests that coastal Antarctic waters were much colder, long before its ice sheet formed.

Contrasting figure 9A and figure 9C, the effect of glacial amplification on GEOCARBSULF datafit is visually evident. With other parameters fixed, larger values of ΔT_{2x} correlate with lower variability in predicted atmospheric CO_2 values. The PDF of model predictions during the late Paleozoic (260-340 Ma) and late Cenozoic (0-40 Ma) glacial intervals varies far less in figure 9C, compared to figure 9A. Proxy CO_2 values in these intervals suffer considerable scatter, but their 10-My means do not vary greatly. This stability of the 10-My-mean proxy-CO_2 values is consistent with a glacial amplification of ΔT_{2x}. As noted above, glacial amplification $GLAC = 2$ does not decrease the lowest possible misfit ($\sim$2.15σ) that GEOCARBSULF can achieve, but it increases the number of independent parameter combinations that can fit the data relatively well.

Perusal of figures 9A, 9B, and 9C suggests that data points near the glacial-interglacial transitions are prominent outliers. One option for improving aggregate GEOCARBSULF data misfit is to extend the "greenhouse" Cenozoic to 30 Ma, and the "icehouse" Paleozoic to 240 Ma, straddling the known environmental transitions at the Antarctic-glaciation onset and the Permo-Triassic boundary. With these alternate glacial intervals, GEOCARBSULF with $GLAC = 2$ continues to misfit Eocene proxy-CO_2 data badly, but greatly improves its match with a 10-My average of three paleosol-based CO_2 estimates from the lower Triassic from Ekart and others (1999) and Prochnow and others (2006), recalibrated according to Breecker and others (2009, 2010) and Gradstein and others (2004), see figure 9D. If the Breecker and others (2010) recalibration is valid for these paleosol data, it could mean that "glacial" climate sensitivities in the long-term carbon cycle can persist for 10 My or more after the ice sheets depart. There are conflicting indicators of the late Permian climate state (Fluteau and others, 2001; Chumakov and Zharkov, 2003; Kiehl and Shields, 2005;

Schneider and others, 2006; Brookfield, 2008), including late-Permian loess deposits (Soreghan and others, 2008) and the persistence of coal depocenters to the 251-Ma Permo-Triassic boundary (Veevers, 2004), However, the scarcity of proxy-CO_2 data in the late-Permian/early-Triassic preclude a full evaluation of this hypothesis.

As an exercise to determine how changes in weatherable land area might explain the major instances of data misfit by GEOCARBSULF, for example, the conjecture of Godderis and others (2008), we altered the boundary condition $f_A(t)$ in the model code. After trial-and-error model runs, we found that a 50 percent decrease in the weatherable continental area in the Jurassic and Eocene improved the datafit substantially (fig. 10). As a practical matter, it strains belief that 50 percent of Earth's land area could be made immune to chemical weathering for these two isolated Phanerozoic intervals, and not at other times in Earth history. We conclude that carbon-cycle factors beyond weatherable-land area must deviate from the values currently used by GEOCARBSULF.

CONCLUSIONS

Our updated climate-sensitivity experiment with the revised GEOCARBSULF and a recalibrated and expanded proxy-CO_2 data set has largely confirmed the results of Royer and others (2007). In addition, we highlight the likelihood that glacial climate sensitivities in the Phanerozoic were amplified by a factor of two or more, relative to non-glacial climate sensitivities. We estimate the empirical probability density function (PDF) of long-term climate sensitivity ΔT_{2x} by summing all distinct parameter choices for the GEOCARBSULF carbon-cycle model with enhanced volcanic weathering (Berner, 2006b, 2008, 2009) that enable the model to fit 10-My averages of 635 recalibrated proxy-CO_2 data for the Phanerozoic within a chosen minimum data-variance reduction, or equivalently, a chosen maximum rms model-data misfit. We estimate an empirical PDF for climate sensitivity from a normalized graph of the proportion of distinct parameter combinations for which GEOCARBSULF meets or exceeds the data-misfit criterion.

Although peaked at its most-probable value near $\Delta T_{2x} = 3°–4$ °C, depending on data-misfit threshold, the width of the empirical PDF for long-term Phanerozoic climate sensitivity ΔT_{2x} is substantial, largely overlapping the ranges for short-term ΔT_{2x} estimated by other researchers using other methods (Knutti and Hegerl, 2008). For all choices of misfit thresholds, the climate sensitivity $\Delta T_{2x}>1.0$ °C with ~99 percent probability, $\Delta T_{2x}>1.5$ °C with ~95 percent probability, and $\Delta T_{2x}>2.0$ °C with ~90 percent probability.

If glacial and nonglacial climate sensitivities are independent and we fix the CO_2 fertilization parameter $FERT = 0.5$, GEOCARBSULF fits the proxy-CO_2 most readily for a glacial amplification $GLAC \geq 2$ and non-glacial $\Delta T_{2x} = 3°–6$ °C. For a specific experiment with $GLAC = 2$ that allows $FERT$ to vary, we infer as most-probable glacial climate sensitivities $\Delta T_{2x}^{(g)} \geq 6°–8$ °C, depending on the misfit threshold. For all choices of misfit thresholds, the glacial climate sensitivity $\Delta T_{2x}^{(g)} > 2.0$ °C with ~99 percent probability, $\Delta T_{2x}^{(g)} > 3.4$ °C with ~95 percent probability, and $\Delta T_{2x}^{(g)} > 4.4$ °C with ~90 percent probability.

We conclude that the GEOCARBSULF climate model, in its present form, is consistent with amplified glacial climate sensitivity due to slow feedbacks (Budyko, 1974, 1982; Hansen and others, 2008), and that the amplification factor is likely to be two or greater. Because the human species lives in a glacial interval of Earth history, this modeling result has more than academic interest. GEOCARBSULF is not a tool to predict climate change accurately on the time scales (decades to centuries) that concern policymakers. The model assumes a long-term balance of carbon fluxes within the Earth system, a condition that is unlikely to be satisfied in the near term. The climate change predicted by our results would take effect only after a significant transition period. Although a precise prediction during the transition period should

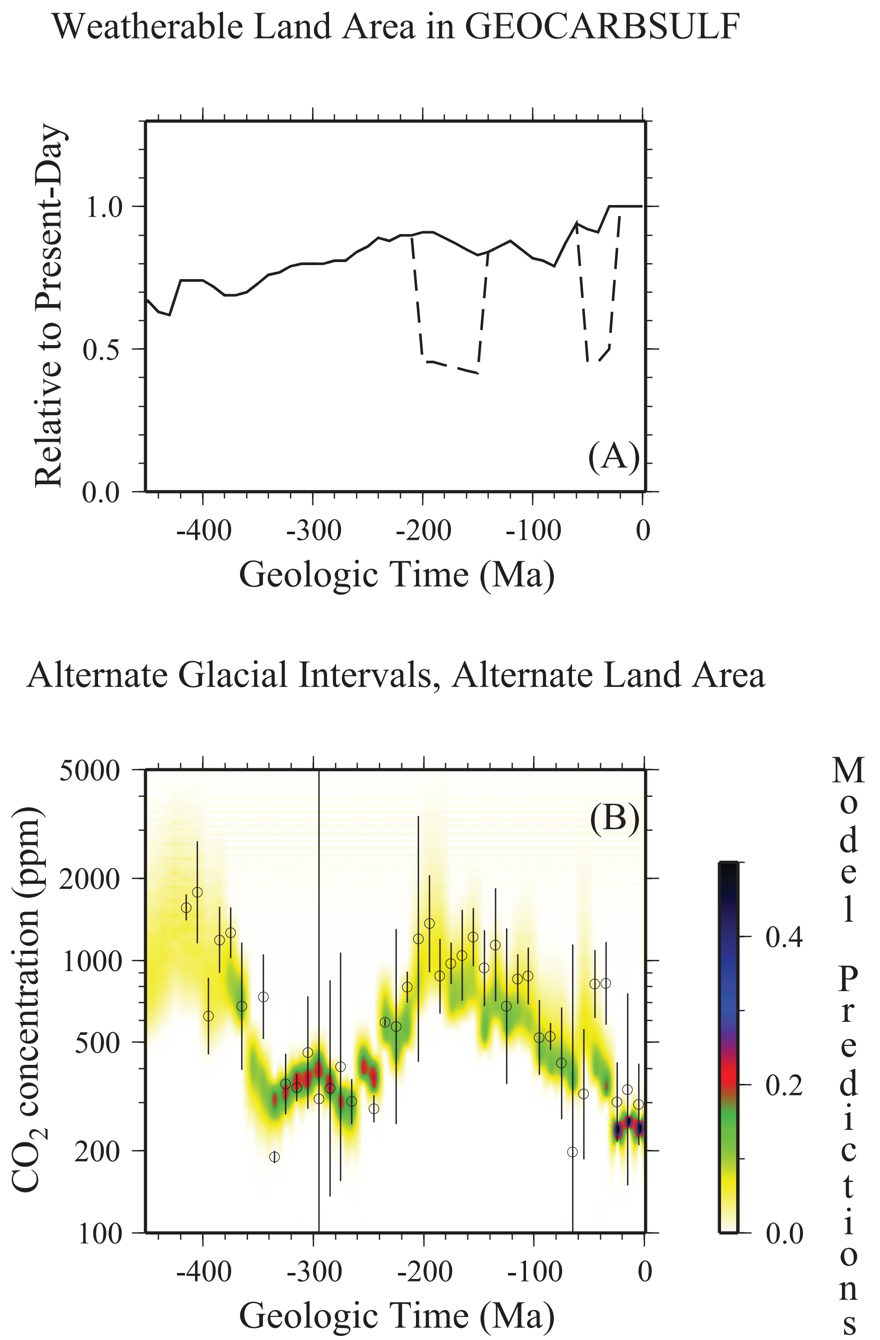

Fig. 10. Thought-experiment for resolving large misfit between proxy-CO_2 data and GEOCARBSULF predictions in the Jurassic (150-200 Ma) and Eocene (30-50 Ma). Panel (A) shows the weatherable land area in GEOCARBSULF proportional to present-day values (solid line) with a hypothetical 50% decrease in the Jurassic and the Eocene. Panel (B) shows the results achieved with this hypothetical decrease in weatherable area, for a glacial climate sensitivity $\Delta T_{2x}^{(g)} = 2\times\Delta T_{2x}$ for 0–30 Ma and 240–340 Ma. Plotting conventions identical to figure 9.

not be inferred from our study, we can conclude with some confidence that the model GEOCARBSULF offers little or no support for the hopeful scenario in which long-term glacial climate sensitivity $\Delta T_{2x}{}^{(g)} < 2$ °C. GEOCARBSULF modeling does lend support to the most recent, and alarming, $\Delta T_{2x}{}^{(g)} = 7$–9 °C estimates for the Plio-Pleistocene (Pagani and others, 2010).

Correlations between ΔT_{2x} and the weathering activation energy parameter *ACT* suggest that high ΔT_{2x} values correlate with low *ACT* values. Low *ACT* values in the literature (Gislason and Oelkers, 2003; Gislason and others, 2009) have been reported for Icelandic volcanic rocks and glasses, and therefore are less probable as a global-average value. After expressing this *a priori* knowledge as a PDF for *ACT*, the long tail of the empirical PDF for ΔT_{2x} dampens somewhat for the case where Phanerozoic climate sensitivity is uniform, that is, no glacial amplification. However, for $GLAC = 2$, the bivariate empirical PDF for ΔT_{2x} and *ACT* peaks at *ACT*-values appropriate for plutonic rocks and minerals (Berner, 2004), so that downweighting low *ACT* values suppresses the high-ΔT_{2x} tail of its empirical PDF less.

The geochemical-cycle model GEOCARBSULF (Berner, 2006b) can fit much of the proxy-CO_2 data well, but proxy-CO_2 data in some time periods are difficult to reconcile. In the Jurassic (150-200 Ma), a 50 percent decrease in weatherable land area greatly improves the data fit, but this reduction is much larger than that suggested by the deep tropical weathering hypothesis of Godderis and others (2008). In the Eocene (30-50 Ma), a similar reduction in weatherable land area and a redefinition of "glacial" climate-sensitivity from 0 to 40 Ma to 0 to 30 Ma improves the datafit somewhat, but not as well as for Jurassic data. For a handful of low-CO_2 estimates near the Permo-Triassic boundary (251 Ma), an extension of late Paleozoic glacial climate sensitivity from 260 to 340 Ma to 240 to 340 Ma improves the datafit substantially, but more observations are needed to justify such an adjustment. Further refinements to GEOCARBSULF may address these shortcomings, and new proxy-CO_2 data may fill gaps and consolidate the time-averaged data. However, carbon-cycle models that treat Earth's surface effectively as a single point are limited. We look forward to similar studies with models that incorporate geographic variability in climate and geochemical processes, for example, Godderis and others (2009), Beaulieu and others (2010).

acknowledgments

Robert A. Berner provided original source code for GEOCARBSULF. Reviewers made helpful comments, particularly a reminder by A. G. Lapenis regarding the Method of Paleoanalogs. JP was supported by the Yale Institute for Biospheric Studies. DLR was supported by other grants.

References

Andrews, J. E., Tandon, S. K., and Dennis, P. F., 1995, Concentration of carbon dioxide in the Late Cretaceous atmosphere: Journal of the Geological Society, v. 152, p. 1–3, doi:10.1144/gsjgs.152.1.0001.

Arrhenius, S., 1896, On the influence of carbonic acid in the air upon the temperature of the ground: Philosophical Magazine, v. 41, p. 237–276, doi:10.1080/14786449608620846.

Arvidson, R. S., MacKenzie, F. T., and Guidry, M., 2006, MAGic: A Phanerozoic model for the geochemical cycling of major rock-forming components: American Journal of Science, v. 306, p. 135–190, doi:10.2475/ajs.306.3.135.

Bala, G., Caldeira, K., Mirin, A., Wickett, M., Delire, C., and Phillips, T. J., 2006, Biogeophysical effects of CO_2 fertilization on global climate: Tellus B, v. 58, p. 620–627, doi:10.1111/j.1600-0889.2006.00210.x.

Bala G., Caldeira, K., Wickett, M., Phillips, T. J., Lobell, D. B., Delire, C., and Mirin, A., 2007, Combined climate and carbon-cycle effects of large-scale deforestation: Proceedings of the National Academy of Sciences of the United States of America, v. 104, p. 6550–6555, doi:10.1073/pnas.0608998104.

Barclay, R. S., McElwain, J. C., and Sageman, B. B., 2010, Carbon sequestration activated by a volcanic CO_2 pulse during Ocean Anoxic Event 2: Nature Geoscience, v. 3, p. 205–208, doi:10.1038/NGEO757.

Beaulieu, E., Godderis, Y., Labat, D., Roelandt, C., Oliva, P., and Guerrero, B., 2010, Impact of atmospheric CO_2 levels on continental silicate weathering: Geochemistry, Geophysics, Geosystems, v. 11, Q07007, doi:10.1029/2010GC003078.

Beerling, D. J., 2002, Low atmospheric CO_2 levels during the Permo-Carboniferous glaciation inferred from fossil lycopsids: Proceedings of the National Academy of Sciences of the United States of America, v. 99, p. 12567–12571, doi:10.1073/pnas.202304999.
Beerling, D. J., and Royer, D. L., 2002, Reading a CO_2 signal from fossil stomata: New Phytologist, v. 153, p. 387–397, doi:10.1046/j.0028-646X.2001.00335.x.
Beerling, D. J., McElwain, J. C., and Osbourne, C. P., 1998, Stomatal responses of the "living fossil" *Ginkgo biloba* L. to changes in atmospheric CO_2 concentrations: Journal of Experimental Botany, v. 49, p. 1603–1607, doi:10.1093/jxb/49.326.1603.
Beerling, D. J., Lomax, B. H., Royer, D. L., Upchurch, G. R., and Kump, L. R., 2002, An atmospheric pCO_2 reconstruction across the Cretaceous-Tertiary boundary from leaf megafossils: Proceedings of the National Academy of Sciences of the United States of America, v. 99, p. 7836–7840, doi:10.1073/pnas.122573099.
Beerling, D. J., Fox, A., and Anderson, C. W., 2009, Quantitative uncertainty analyses of ancient atmospheric CO_2 estimates from fossil leaves: American Journal of Science, v. 309, p. 775–787, doi:10.2475/09.2009.01.
Bergman, N. M., Lenton, T. M., and Watson, A. J., 2004, COPSE: A new model of biogeochemical cycling over Phanerozoic time: American Journal of Science, v. 304, p. 397–437, doi:10.2475/ajs.304.5.39.
Berner, R. A., 1991, A model for atmospheric CO_2 over Phanerozoic time: American Journal of Science, v. 291, p. 339–376, doi:10.2475/ajs.291.4.339.
——— 1994, GEOCARB-II: A revised model of atmospheric CO_2 over Phanerozoic time: American Journal of Science, v. 294, p. 56–91, doi:10.2475/ajs.294.1.56.
——— 2001, Modeling atmospheric O_2 over Phanerozoic time: Geochimica et Cosmochimica Acta, v. 65, p. 685–694, doi:10.1016/S0016-7037(00)00572-X.
——— 2004, The Phanerozoic Carbon Cycle: CO_2 and O_2: New York, Oxford University Press, 150 p.
——— 2006a, GEOCARBSULF: A combined model for Phanerozoic atmospheric O_2 and CO_2: Geochimica et Cosmochimica Acta, v. 70, p. 5653–5664, doi:10.1016/j.gca.2005.11.032.
——— 2006b, Inclusion of the weathering of volcanic rocks in the GEOCARBSULF model: American Journal of Science, v. 306, p. 295–302, doi:10.2475/052006.01.
——— 2008, Addendum to "Inclusion of the weathering of volcanic rocks in the GEOCARBSULF model": (R. A. Berner, 2006, v. 306, p. 295–302): American Journal of Science, v. 308, p. 100–103, doi:10.2475/01.2008.04.
——— 2009, Phanerozoic atmospheric oxygen: New results using the GEOCARBSULF Model: American Journal of Science, v. 309, p. 603–606, doi:10.2475/07.2009.03.
Berner, R. A., and Kothavala, Z., 2001, GEOCARB III: A revised model of atmospheric CO_2 over Phanerozoic time: American Journal of Science, v. 301, p. 182–204, doi:10.2475/ajs.301.2.182.
Berner, R. A., Lasaga, A. C., and Garrels, R. M., 1983, The carbonate-silicate geochemical cycle and its effect on atmospheric carbon dioxide over the past 100 million years: American Journal of Science, v. 283, p. 641–683, doi:10.2475/ajs.283.7.641.
Berner, R. A., VandenBrooks, J. M., and Ward, P. D., 2007, Oxygen and evolution: Science, v. 316, p. 557–558, doi:10.1126/science.1140273.
Boé, J., Hall, A., and Qu, X., 2009, Current GCMs' unrealistic negative feedback in the Arctic: Journal of Climate, v. 22, p. 4682–4695, doi:10.1175/2009JCLI2885.1.
Borzenkova, I. I., 2003, Determination of global climate sensitivity to the gas composition of the atmosphere from paleoclimatic data: Izestiya Atmospheric and Oceanic Physics, v. 39, p. 197–202.
Breecker, D. O., Sharp, Z. D., and McFadden, L. D., 2009, Seasonal bias in the formation and stable isotopic composition of pedogenic carbonate in modern soils from central New Mexico, USA: Geological Society of America Bulletin, v. 121, p. 630–640, doi:10.1130/B26413.1.
——— 2010, Atmospheric CO_2 concentrations during ancient greenhouse climates were similar to those predicted for A.D. 2100: Proceedings of the National Academy of Sciences of the United States of America, v. 107, p. 576–580, doi:10.1073/pnas.0902323106.
Brookfield, M. E., 2008, Palaeoenvironments and palaeotectonics of the arid to hyperarid intracontinental latest Permian–late Triassic Solway basin (U.K.): Sedimentary Geology, v. 210, p. 27–47, doi:10.1016/j.sedgeo.2008.06.003.
Budyko, M. I., 1974, Climate and Life: New York, Academic Press, 495 p.
——— 1982, The Earth's Climate: Past and Future: New York, Academic Press, 304 p.
Cerling, T. E., 1991, Carbon dioxide in the atmosphere: Evidence from Cenozoic and Mesozoic paleosols: American Journal of Science, v. 291, p. 377–400, doi:10.2475/ajs.291.4.377.
——— 1992, Use of carbon isotopes in paleosols as an indicator of the pCO_2 of the paleoatmosphere: Global Biogeochemical Cycles, v. 6, p. 307–314, doi:10.1029/92GB01102.
Chen, L. Q., Li, C. S., Chaloner, W. G., Beerling, D. J., Sun, Q. G., Collinson, M. E., and Mitchell, P. L., 2001, Assessing the potential for the stomatal characters of extant and fossil *Ginkgo* leaves to signal atmospheric CO_2 change: American Journal of Botany, v. 88, p. 1309–1315.
Chumakov, N. M., and Zharkov, M. A., 2003, Climate during the Permian-Triassic biosphere reorganizations. Article 2. Climate of the Late Permian and Early Triassic: General inferences: Stratigraphical and Geological Correlation, v. 11, p. 361–375.
Cleveland, D. M., Nordt, L. C., Dworkin, S. I., and Atchley, S. C., 2008, Pedogenic carbonate isotopes as evidence for extreme climatic events preceding the Triassic-Jurassic boundary: Implications for the biotic crisis?: Geological Society of America Bulletin, v. 120, p. 1408–1415; doi:10.1130/B26332.1.
Cox, J. E., Railsback, L. B., and Gordon, E. A., 2001, Evidence from Catskill pedogenic carbonates for a rapid large Devonian decrease in atmospheric carbon dioxide concentrations: Northeastern Geology and Environmental Sciences, v. 23, p. 91–102.
Crowley, T. J., 1997, The problem of paleo-analogues: Climatic Change, v. 35, p. 119–121, doi:10.1023/A:1005372427022.

——— 1998, Significance of tectonic boundary conditions for paleoclimate simulations, *in* Crowley, T. J., and Burke, K., editors, Tectonic Boundary Conditions for Climate Reconstructions: New York, Oxford University Press, p. 3–17.

DeConto, R. M., and Pollard, D., 2003, Rapid Cenozoic glaciation of Antarctica induced by declining atmospheric CO_2: Nature, v. 421, p. 245–249, doi:10.1038/nature01290.

Dessert, C., Dupré, B., Francois, L. M., Schott, J., Gaillardet, J., Chakrapani, G., and Bajpai, S., 2001, Erosion of Deccan Traps determined by river geochemistry: Impact on the global climate and the $^{87}Sr/^{86}Sr$ ratio of seawater: Earth and Planetary Science Letters, v. 188, p. 459–474, doi:10.1016/S0012-821X(01)00317-X.

Dessert, C., Dupré, B., Gaillardet, J., Francois, L. M., and Allegre, C. J., 2003, Basalt weathering laws and the impact of basalt weathering on the global carbon cycle: Chemical Geology, v. 202, p. 257–273, doi:10.1016/j.chemgeo.2002.10.001.

Dinha, A., and Stott, L. D., 1994, New atmospheric pCO_2 estimates from paleosols during the late Paleocene/early Eocene global warming interval: Global and Planetary Change, v. 9, p. 297–307, doi:10.1016/0921-8181(94)00010-7.

Doria, G., Royer, D. L., Wolfe, A. P., Fox, A., Westgate, J., and Beerling, D. J., 2011, Declining atmospheric CO_2 during the late middle Eocene climate transition (40 Ma), American Journal of Science, v. 311, p. 63–75, doi:10.2745/01.2011.03.

Driese, S. G., Mora, C. I., and Elick, J. M., 2000, The paleosol record of increasing plant diversity and depth of rooting and changes in atmospheric pCO_2 in the Siluro-Devonian, *in* Gastaldo, R. A., and DiMichele, W. A., editors, Phanerozoic Terrestrial Ecosystems: New Haven, Short Course, The Paleontological Society Special Publication, v. 6, p. 47–61.

Ebelmen, J. J., 1845, Sur les produits de la decomposition des especes minerales de la familie des silicates: Annales des Mines, v. 7, p. 3–66.

Ekart, D. D., Cerling, T. E., Montañez, I. P., and Tabor, N. J., 1999, A 400 million year carbon isotope record of pedogenic carbonate: Implications for paleoatmospheric carbon dioxide: American Journal of Science, v. 299, p. 805–827, doi:10.2475/ajs.299.10.805.

Falkowski, P. G., Katz, M. E., Milligan, A. J., Fennel, K., Cramer, B. S., Aubry, M. P., Berner, R. A., Novacek, M. J., and Zapol, W. M., 2005, The rise of oxygen over the past 205 million years and the evolution of large placental mammals: Science, v. 309, p. 2202–2204, doi:10.1126/science.1116047.

Fielding, C. R., Frank, T. D., and Isbell, J. L., 2008, The late Paleozoic ice age: A review of current understanding and synthesis of global climate patterns, *in* Fielding, C. R., Frank, T. D., and Isbell, J. L., editors, Resolving the Late Paleozoic Ice Age in Time and Space: GSA Special Paper, v. 441, p. 343–354, doi:10:1130/2008.2441(24).

Fletcher, B. J., Brentnall, S. J., Anderson, C. W., Berner, R. A., and Beerling, D. J., 2008, Atmospheric carbon dioxide linked with Mesozoic and early Cenozoic climate change: Nature Geoscience, v. 1, p. 43–48, doi:10.1038/ngeo.2007.29.

Fluteau, F., Besse, J., Broutin, J., and Ramstein, G., 2001, The Late Permian climate. What can be inferred from climate modelling concerning Pangea scenarios and Hercynian range altitude?: Palaeogeography Palaeoclimatology Palaeoecology, v. 167, p. 39–71, doi:10.1016/S0031-0182(00)00230-3.

Forest, C. E., Stone, P. H., Sokolov, A. P., Allen, M. R., and Webster, M. D., 2002, Quantifying uncertainties in climate system properties with the use of recent climate observations: Science, v. 295, p. 113–117, doi:10.1126/science.1064419.

Franks, P. J., and Beerling, D. J., 2009, CO_2 forced evolution of plant gas exchange capacity and water-use efficiency over the Phanerozoic: Geobiology, v. 7, p. 227–236, doi:10.1111/j.1472-4669.2009.00193.x.

Freeman, K. H., and Hayes, J. M., 1992, Fractionation of carbon isotopes by phytoplankton and estimates of ancient CO_2 levels: Global Biogeochemical Cycles, v. 6, p. 185–198, doi:10.1029/92GB00190.

Garrels, R. M., and Lerman, A., 1984, Coupling of the sedimentary sulfur and carbon cycles—An improved model: American Journal of Science, v. 284, p. 989–1007, doi:10.2475/ajs.284.9.989.

Ghosh, P., Bhattacharya, S. K., and Jani, R. A., 1995, Palaeoclimate and palaeovegetation in central India during the Upper Cretaceous based on stable isotope composition of the palaeosol carbonates: Palaeogeography Palaeoclimatology Palaeoecology, v. 114, p. 285–296, doi:10.1016/0031-0182(94)00082-J.

Ghosh, P., Ghosh, P., and Bhattacharya, S. K., 2001, CO_2 levels in the Late Palaeozoic and Mesozoic atmosphere from soil carbonate and organic matter, Satpura basin, Central India: Palaeogeography Palaeoclimatology Palaeoecology, v. 170, p. 219–236, doi:10.1016/S0031-0182(01)00237-1.

Ghosh, P., Bhattacharya, S. K., and Ghosh, P., 2005, Atmospheric CO_2 during the Late Paleozoic and Mesozoic: Estimates from Indian soils, *in* Ehleringer, J. R., Cerling, T. E., and Dearing, M. D., editors, A History of Atmospheric CO_2 and Its Effects on Plants, Animals, and Ecosystems: New York, Springer, Ecological Studies, v. 177, p. 8–34.

Gislason, S. R., and Oelkers, E. H., 2003, Mechanism, rates, and consequences of basaltic glass dissolution: II. An experimental study of the dissolution rates of basaltic glass as a function of pH and temperature: Geochimica et Cosmochimica Acta, v. 67, p. 3817–3832, doi:10.1016/S0016-7037(03)00176-5.

Gislason, S. R., Oelkers, E. H., Eiriksdottir, E. S., Kardjilov, M. I., Gisladottir, G., Sigfusson, B., Snorrason, A., Elefsen, S., Hardardottir, J., Torssander, P., and Oskarsson, N., 2009, Direct evidence of the feedback between climate and weathering: Earth and Planetary Science Letters, v. 277, p. 213–222, doi:10.1016/j.epsl.2008.10.018.

Godderis, Y., Donnadieu, Y., Tombozafy, M., and Dessert, C., 2008, Shield effect on continental weathering: Implication for climatic evolution of the Earth at the geological timescale: Geoderma, v. 145, p. 439–448, doi:10.1016/j.geoderma.2008.01.020.

Godderis, Y., Roelandt, C., Schott, J., Perret, M. C., and Francois, L. M., 2009, Towards an integrated model of weathering, climate and biospheric processes: Reviews in Mineralogy and Geochemistry, v. 70, p. 411–434, doi:10.2138/rmg.2009.70.9.

Gradstein, F. M., Ogg, J. G., and Smith, A. G., 2004, A Geological Timescale 2004: Cambridge, Cambridge University Press, 589 p.

Greenwood, D. R., Scarr, M. J., and Christophel, D. C., 2003, Leaf stomatal frequency in the Australian tropical rainforest tree *Neolitsea dealbata* (Lauraceae) as a proxy measure of atmospheric pCO_2: Palaeogeography Palaeoclimatology Palaeoecology, v. 196, p. 375–393, doi:10.1016/S0031-0182(03)00465-6.

Hansen, J., Sato, M., Kharecha, P., Beerling, D., Berner, R., Masson-Delmotte, V., Pagani, M., Raymo, M., Royer, D. L., and Zachos, J. C., 2008, Target atmospheric CO_2: Where should humanity aim?: Open Atmospheric Science Journal, v. 2, p. 217–231, doi:10.2174/1874282300802010217.

Haworth, M., Hesselbo, S. P., McElwain, J. C., Robinson, S. A., and Brunt, J. W., 2005, Mid-Cretaceous pCO_2 based on stomata of the extinct conifer *Pseudofrenelopsis* (Cheirolepidiaceae): Geology, v. 33, p. 749–752, doi:10.1130/G21736.1.

Hegerl, G. C., Crowley, T. J., Hyde, W. T., and Frame, D. J., 2006, Climate sensitivity constrained by temperature reconstructions over the past seven centuries: Nature, v. 440, p. 1029–1032, doi:10.1038/nature04679.

Higgins, J. A., and Schrag, D. P., 2006, Beyond methane: Towards a theory for the Paleocene-Eocene Thermal Maximum: Earth and Planetary Science Letters, v. 245, p. 523–537, doi:10.1016/j.epsl.2006.03.009.

Hoffert, M. I., and Covey, C., 1992, Deriving global climate sensitivity from paleoclimate reconstructions: Nature, v. 360, p. 573–576, doi:10.1038/360573a0.

IPCC, 2007, Climate Change 2007: The Physical Science Basis, *in* Solomon, S., Qin, D., Manning, M., Chen, Z., Marquis, M., Averyt, K. B., Tignor, M., and Miller, H. L., editors, Contribution of Working Group I to the Fourth Assessment Report of the Intergovernmental Panel on Climate Change: Cambridge, Cambridge University Press, 996 p.

Kheshgi, H. S., Schlesinger, M. E., and Lapenis, A. G., 1997, Comparison of paleotemperature reconstructions as evidence for the Paleo-Analog Hypothesis: Climatic Change, v. 35, p. 123–131, doi:10.1023/A:1005348309505.

Kiehl, J. T., and Shields, C. A., 2005, Climate simulation of the latest Permian: Implications for mass extinction: Geology, v. 33, p. 757–760, doi:10.1130/G21654.1.

Knutti, R., and Hegerl, G. C., 2008, The equilibrium sensitivity of the Earth's temperature to radiation changes: Nature Geoscience, v. 1, p. 735–743, doi:10.1038/ngeo337.

Koch, P. L., Zachos, J. C., and Gingerich, P. D., 1992, Correlation between isotope records in marine and continental carbon reservoirs near the Palaeocene/Eocene boundary: Nature, v. 358, p. 319–322, doi:10.1038/358319a0.

Kürschner, W. M., Kvacek, Z., and Dilcher, D. L., 2008, The impact of Miocene atmospheric carbon dioxide fluctuations on climate and the evolution of terrestrial ecosystems: Proceedings of the National Academy of Sciences of the United States of America, v. 105, p. 449–453, doi:10.1073/pnas.0708588105.

Lear, C. H., Elderfield, H., and Wilson, P. A., 2000, Cenozoic deep-sea temperatures and global ice volumes from Mg/Ca in benthic foraminiferal calcite: Science, v. 287, p. 269–272, doi:10.1126/science.287.5451.269.

Lee, Y. I., 1999, Stable isotopic composition of calcic paleosols of the Early Cretaceous Hasandong Formation, southeastern Korea: Palaeogeography Palaeoclimatology Palaeoecology, v. 150, p. 123–133, doi:10.1016/S0031-0182(99)00010-3.

Lee, Y. I., and Hisada, K., 1999, Stable isotopic composition of pedogenic carbonates of the Early Cretaceous Shimonoseki Subgroup, western Honshu, Japan: Palaeogeography Palaeoclimatology Palaeoecology, v. 153, p. 127–138, doi:10.1016/S0031-0182(99)00069-3.

Liu, Z., Pagani, M., Zinniker, D., DeConto, R., Huber, M., Brinkhuis, H., Shah, S. R., Leckie, R. M., and Pearson, A., 2009, Global cooling during the Eocene-Oligocene climate transition: Science, v. 323, p. 1187–1190, doi:10.1126/science.1166368.

Lunt, D. J., Haywood, A. M., Schmidt, G. A., Salzmann, U., Valdes, P. J., and Dowsett, H. J., 2010, Earth system sensitivity inferred from Pliocene modelling and data: Nature Geoscience, v. 3, p. 60–64, doi:10.1038/ngeo706.

Lyell, C., 1837, Principles of Geology, An Inquiry How Far the Former Changes of the Earth's Surface are Referable to Causes now in Operation, Volume 1: Pittsburgh, John Kay & Co, 551 p.

Manabe, S., and Wetherald, R. T., 1967, Thermal equilibrium of the atmosphere with a given distribution of relative humidity: Journal of Atmospheric Sciences, v. 24, p. 241–259.

McElwain, J. C., 1998, Do fossil plants signal palaeoatmospheric CO_2 concentration in the geological past?: Philosophical Transactions of the Royal Society of London, Series B, v. 353, p. 83–96, doi:10.1098/rstb.1998.0193.

McElwain, J. C., Beerling, D. J., and Woodward, F. I., 1999, Fossil plants and global warming at the Triassic-Jurassic boundary: Science, v. 285, p. 1386–1390, doi:10.1126/science.285.5432.1386.

Meybeck, M., 1987, Global chemical weathering of surficial rocks estimated from river-dissolved loads: American Journal of Science, v. 287, p. 401–428, doi:10.2475/ajs.287.5.401.

Montañez, I. P., Tabor, N. J., Niemeier, D., DiMichele, W. A., Frank, T. D., Fielding, C. R., Isbell, J. L, Birgenheier, L. P., and Rygel, M. C., 2007, CO_2-forced climate and vegetation instability during late Paleozoic deglaciation: Science, v. 315, p. 87–91; doi:10.1126/science.1134207.

Mora, C. I., Driese, S. G., and Colarusso, L. A., 1996, Middle to Late Paleozoic atmospheric CO_2 levels from soil carbonate and organic matter: Science, v. 271, p. 1105–1107, doi:10.1126/science.271.5252.1105.

Moulton, K. L., West, J., and Berner, R. A., 2000, Solute flux and mineral mass balance approaches to the quantification of plant effects on silicate weathering: American Journal of Science, v. 300, p. 539–570, doi:10.2475/ajs.300.7.539.

Muchez, P., Peeters, C., Keppens, E., and Viaene, W. A., 1993, Stable isotopic composition of paleosols in the Lower Viséan of eastern Belgium: Evidence of evaporation and soil-gas CO_2: Chemical Geology, v. 106, p. 389–396, doi:10.1016/0009-2541(93)90039-L.

Nordt, L., Atchley, S., and Dworkin, S. I., 2002, Paleosol barometer indicates extreme fluctuations in atmospheric CO_2 across the Cretaceous-Tertiary boundary: Geology, v. 30, p. 703–706, doi:10.1130/0091-7613(2002)030⟨0703:PBIEFI⟩2.0.CO;2.

——— 2003, Terrestrial evidence for two greenhouse events in the latest Cretaceous: GSA Today, v. 13, p. 4–9, doi:10.1130/1052-5173(2003)013⟨4:TEFTGE⟩2.0.CO;2.

Pagani, M., Arthur, M. A., and Freeman, K. H., 1999a, Miocene evolution of atmospheric carbon dioxide: Paleoceanography, v. 14, p. 273–292, doi:10.1029/1999PA900006.

Pagani, M., Freeman, K. H., and Arthur, M. A., 1999b, Late Miocene atmospheric CO_2 concentrations and the expansion of C4 grasses: Science, v. 285, p. 876–879, doi:10.1126/science.285.5429.876.

Pagani, M., Zachos, J. C., Freeman, K. H., Tipple, B., and Bohaty, S., 2005, Marked decline in atmospheric carbon dioxide concentrations during the Paleogene: Science, v. 309, p. 600–603, doi:10.1126/science.1110063.

Pagani, M., Caldeira, K., Archer, D., and Zachos, J. C., 2006, An ancient carbon mystery: Science, v. 314, p. 1556–1557, doi:10.1126/science.1136110.

Pagani, M., Liu, Z., LaRiviere, J., and Ravelo, A. C., 2010, High Earth-system climate sensitivity determined from Pliocene carbon dioxide concentrations: Nature Geoscience, v. 3, p. 27–30, doi:10.1038/ngeo724.

Passalia, M. G., 2009, Cretaceous pCO_2 estimation from stomatal frequency analysis of gymnosperm leaves of Patagonia, Argentina: Palaeogeography Palaeoclimatology Palaeoecology, v. 273, p. 17–24, doi:10.1016/j.palaeo.2008.11.010.

Pearson, P. N., and Palmer, M. R., 2000, Atmospheric carbon dioxide concentrations over the past 60 million years: Nature, v. 406, p. 695–699, doi:10.1038/35021000.

Pearson, P. N., van Dongen, B. E., Nicholas, C. J., Pancost, R. D., Schouten, S., Singano, J. M., and Wade, B. S., 2007, Stable warm tropical climate through the Eocene Epoch: Geology, v. 35, p. 211–214, doi:10.1130/G23175A.1.

Pearson, P. N., Foster, G. L., and Wade, B. S., 2009, Atmospheric carbon dioxide through the Eocene-Oligocene climate transition: Nature, v. 461, p. 1110–1114, doi:10.1038/nature08447.

Peters, S. E., Carlson, A. E., Kelly, D. C., and Gingerich, P. D., 2010, Large-scale glaciation and deglaciation of Antarctica during the Late Eocene: Geology, v. 38, p. 723–726, doi:10.1130/G31068.1.

Platt, N. H., 1989, Continental sedimentation in an evolving rift basin: the Lower Cretaceous of the western Cameros Basin (northern Spain): Sedimentary Geology, v. 64, p. 91–109, doi:10.1016/0037-0738(89)90086-9.

Prochnow, S. J., Nordt, L. C., Atchley, S. C., and Hudec, M. R., 2006, Multi-proxy paleosol evidence for middle and late Triassic climate trends in eastern Utah: Palaeogeography Palaeoclimatology Palaeoecology, v. 232, p. 53–72, doi:10.1016/j.palaeo.2005.08.011.

Quan, C., Sun, C., Sun, Y., and Sun, G., 2009, High resolution estimates of paleo-CO_2 levels through the Campanian (Late Cretaceous) based on *Ginkgo* cuticles: Cretaceous Research, v. 30, p. 424–428, doi:10.1016/j.cretres.2008.08.004.

Randall, D. A., Wood, R. A., Bony, S., Colman, R., Fichefet, T., Fyfe, J., Kattsov, V., Pitman, A., Shukla, J., Srinivasan, J., Stouffer, R. J., Sumi, A., and Taylor, K. E., 2007, Climate models and their evaluation, *in* Solomon, S., Qin, D., Manning, M., Chen, Z., Marquis, M., Averyt, K. B., Tignor, M., and Miller, H. L., editors, Climate Change 2007: The Physical Science Basis. Contribution of Working Group I to the Fourth Assessment Report of the Intergovernmental Panel on Climate Change: Cambridge, Cambridge University Press, p. 589–662.

Raymo, M. E., and Ruddiman, W. F., 1992, Tectonic forcing of late Cenozoic climate: Nature, v. 359, p. 117–122, doi:10.1038/359117a0.

Retallack, G. J., 2003, Soils and Global Change in the Carbon Cycle over Geological Time, *in* Drever, J. I., editor, Surface and Ground Water, Weathering, and Soils: Amsterdam, Elsevier, Treatise on Geochemistry, v. 5, p. 1–6, doi:10.1016/B0-08-043751-6/05087-8.

——— 2009a, Greenhouse crises of the past 300 million years: Geological Society of America Bulletin, v. 121, p. 1441–1455, doi:10.1130/B26341.1.

——— 2009b, Refining a pedogenic-carbonate CO_2 paleobarometer to quantify a middle Miocene greenhouse spike: Palaeogeography Palaeoclimatology Palaeoecology, v. 281, p. 57–65, doi:10.1016/j.palaeo.2009.07.011.

Robinson, S. A., Andrews, J. E., Hesselbo, S. P., Radley, J. D., Dennis, P. F., Harding, I. C., and Allen, P., 2002, Atmospheric pCO_2 and depositional environment from stable-isotope geochemistry of calcrete nodules (Barremian, Lower Cretaceous, Wealden Beds, England): Journal of the Geological Society, London, v. 159, p. 215–224, doi:10.1144/0016-764901-015.

Roth-Nebelsick, A., and Konrad, W., 2003, Assimilation and transpiration capabilities of rhyniophytic plants from the Lower Devonian and their implications for paleoatmospheric CO_2 concentration: Palaeogeography Palaeoclimatology Palaeoecology, v. 202, p. 153–178, doi:10.1016/S0031-0182(03)00634-5.

Royer, D. L., 2006, CO_2-forced climate thresholds during the Phanerozoic: Geochimica et Cosmochimica Acta, v. 70, p. 5665–5675, doi:10.1016/j.gca.2005.11.031.

——— 2010, Fossil soils constrain ancient climate sensitivity: Proceedings of the National Academy of Sciences of the United States of America, v. 107, p. 517–518, doi:10.1073/pnas.0913188107.

Royer, D. L., Berner, R. A., and Beerling, D. J., 2001, Phanerozoic atmospheric CO_2 change: Evaluating geochemical and paleobiological approaches: Earth-Science Reviews, v. 54, p. 349–392, doi:10.1016/S0012-8252(00)00042-8.

Royer, D. L., Berner, R. A., Montañez, I. P., Tabor, N. J., and Beerling, D. J., 2004, CO_2 as a primary driver of Phanerozoic climate: GSA Today, v. 14, p. 4–10, doi:10.1130/1052-5173(2004)014⟨4:CAAPDO⟩2.0.CO;2.

Royer, D. L., Berner, R. A., and Park, J., 2007, Climate sensitivity constrained by CO_2 concentrations over the last 420 million years: Nature, v. 446, p. 530–532, doi:10.1038/nature05699.

Schneider, J. W., Körner, F., Roscher, M., and Kroner, U., 2006, Permian climate development in the northern peri-Tethys area—The Lodève basin, French Massif Central, compared in a European and global context: Palaeogeography Palaeoclimatology Palaeoecology, v. 240, p. 161–183, doi:10.1016/j.palaeo.2006.03.057.

Shabalova, M. V., and Können, G. P., 1995, Climate change scenarios: Comparisons of paleoreconstructions with recent temperature changes: Climatic Change, v. 29, p. 409–428, doi:10.1007/BF01092426.

Siegenthaler, U., Stocker, T. F., Monnin, E., Luthi, D., Schwander, J., Stauffer, B., Raynaud, D., Barnola, J.-M., Fischer, H., Masson-Delmotte, V., and Jouzel, J., 2005, Stable carbon cycle-climate relationship during the late Pleistocene: Science, v. 310, p. 1313–1317, doi:10.1126/science.1120130.

Sinha, A., and Stott, L. D., 1994, New atmospheric *p*CO2 estimates from palesols during the late Paleocene/early Eocene global warming interval: Global and Planetary Change, v. 9, p. 297–307, doi:10.1016/0921-8181(94)00010-7.

Sloan, L. C., and Rea, D. K., 1995, Atmospheric carbon dioxide and early Eocene climate: A general circulation modeling sensitivity study: Palaeogeography Palaeoclimatology Palaeoecology, v. 119, p. 275–292, doi:10.1016/0031-0182(95)00012-7.

Smith, M. E., Carroll, A. R., and Mueller, E. R., 2009, Elevated weathering rates in the Rocky Mountains during the Early Eocene Climatic Optimum: Nature Geoscience, v. 1, p. 370–374, doi:10.1038/ngeo205.

Soreghan, G. S., Soreghan, M. J., and Hamilton, M. A., 2008, Origin and significance of loess in late Paleozoic western Pangaea: A record of tropical cold?: Palaeogeography Palaeoclimatology Palaeoecology, v. 268, p. 234–259, doi:10.1016/j.palaeo.2008.03.050.

Stott, L. D., 1992, Higher temperatures and lower oceanic pCO_2: a climate enigma at the end of the Paleocene Epoch: Paleoceanography, v. 7, p. 395–404, doi:10.1029/92PA01183.

Suchecki, R. K., Hubert, J. F., and de Wet, C. B., 1988, Isotopic imprint of climate and hydrogeochemistry on terrestrial strata of the Triassic-Jurassic Hartford and Fundy rift basins: Journal of Sedimentary Petrology, v. 58, p. 801–811, doi:10.1306/212F8E6D-2B24-11D7-8648000102C1865D.

Sun, B. N., Xiao, L., Xie, S. P., Deng, S. H., Wang, Y. D., Jia, H., and Turner, S., 2007, Quantitative analysis of paleoatmospheric CO_2 level based on stomatal characters of fossil *Ginkgo* from Jurassic to Cretaceous in China: Acta Geologica Sinica (Beijing), v. 81, p. 931–939.

Tabor, N. J., Yapp, C. J., and Montañez, I. P., 2004, Goethite, calcite, and organic matter from Permian and Triassic soils: Carbon isotopes and CO_2 concentrations: Geochimica et Cosmochimica Acta, v. 68, p. 1503–1517, doi:10.1016/S0016-7037(03)00497-6.

Tanner, L. H., Hubert, J. F., Coffey, B. P., and McInerney, D. P., 2001, Stability of atmospheric CO_2 levels across the Triassic/Jurassic boundary: Nature, v. 411, p. 675–677, doi:10.1038/35079548.

Taylor, A. S., ms, 2000, Chemical weathering rates and Sr isotopes: New Haven, Connecticut, Yale University, Ph. D. thesis, 240 p.

Taylor, A. S., Lasaga, A. C., and Blum, J. D., 1999, Effect of lithology on silicate weathering rates, *in* Armannsson, H., editor, Geochemistry of the Earth Surface: Rotterdam, Balkema, p. 127–128.

Tong, J. A., You, Y., Muller, R. D., and Seton, M., 2009, Climate model sensitivity to atmospheric CO_2 concentrations for the middle Miocene: Global and Planetary Change, v. 67, p. 129–140, doi:10.1016/j.gloplacha.2009.02.001.

Tripati, A. K., Roberts, C. D., and Eagle, R. A., 2009, Coupling of CO_2 and ice sheet stability over major climate transitions of the last 20 million years: Science, v. 326, p. 1394–1398, doi:10.1126/science.1178296.

Urban, N. M., and Keller, K., 2009, Complementary observational constraints on climate sensitivity: Geophysical Research Letters, v. 36, L04708, doi:10.1029/2008GL036457.

Van der Burgh, J., Visscher, H., Dilcher, D. L., and Kürschner, W. M., 1993, Paleoatmospheric signatures in Neogene fossil leaves: Science, v. 260, p. 1788–1790, doi:10.1126/science.260.5115.1788.

Veevers, J. J., 2004, Gondwanaland from 650–500 Ma assembly through 320 Ma merger in Pangea to 185–100 Ma breakup: Supercontinental tectonics via stratigraphy and radiometric dating: Earth-Science Reviews, v. 68, p. 1–132, doi:10.1016/j.earscirev.2004.05.002.

Wallmann, K., 2001, Controls on the Cretaceous and Cenozoic evolution of seawater composition, atmospheric CO_2 and climate: Geochimica et Cosmochimica Acta, v. 65, p. 3005–3025, doi:10.1016/S0016-7037(01)00638-X.

Wigley, T. M. L., Jones, P. D., and Raper, S. C. B., 1997, The observed global-warming record: What does it tell us?: Proceedings of the National Academy of Sciences of the United States of America, v. 94, p. 8314–8320, doi:10.1073/pnas.94.16.8314.

Yan, D. F., Sun, B. N., Xie, S. P., Li, X. C., and Wen, W. W., 2009, Response to paleoatmospheric CO_2 concentration of *Solenites vimineus* (Phillips) Harris (Ginkgophyta) from the Middle Jurassic of the Yaojie Basin, Gansu Province, China: Science in China Series D: Earth Sciences, v. 52, p. 2029–2039, doi:10.1007/s11430-009-0181-1.

Zachos, J. C., Opdyke, B. N., Quinn, T. M., Jones, C. E., and Halliday, A. N., 1999, Early Cenozoic glaciation, Antarctic weathering, and seawater $^{87}Sr/^{86}Sr$: Is there a link?: Chemical Geology, v. 161, p. 165–180, doi:10.1016/S0009-2541(99)00085-6.

Zachos, J., Pagani, M., Sloan, L., Thomas, E., and Billups, K., 2001, Trends, rhythms and aberrations in global climate 65 Ma to present: Science, v. 292, p. 686–693, doi:10.1126/science.1059412.

Zachos, J. C., Dickens, G. R., and Zeebe, R. E., 2008, An early Cenozoic perspective on greenhouse warming and carbon-cycle dynamics: Nature, v. 451, p. 279–283, doi:10.1038/nature06588.

Zubakov, V. A., and Borzenkova, I. I., 1990, Global Paleoclimate of the Late Cenozoic: Amsterdam, Elsevier, Developments in Palaeontology and Stratigraphy, v. 12, 456 p.